Strong and Weak Lensing Studies at Fermilab

Elizabeth Buckley-Geer
Experimental Astrophysics Group
Fermilab Center for Particle Astrophysics

Outline

- Lensing 101
  - Strong Lensing
  - Weak Lensing
- Strong lensing systems in SDSS and BCS data
- Weak Lensing measurements in SDSS and BCS data
- Future plans
- Summary

Collaborators

- Fermilab: H. Lin, D. Kubik, H.T. Diehl, S. Allam, D. Tucker, E. Buckley-Geer, J. Kubo, J. Annis, J. Frieman, D. Finley, J. Estrada, D. McGinnis, V. Scarpine, Emily Drabek (intern) … Fermilab Cosmology Analysis Group

- IMSA Students: Liana Nicklaus, Anderson West, Dylan Nelson, Tony Yunker

- Other Institutions: D. Schneider, M. Oguri, A. Shapley, A. Baker, D. Lutz, J.A. Smith, J. Brinchmann, M. Strauss, M.-S. Shin, C. Kochanek, C. Tremonti, …

What is Gravitational Lensing

- General Relativity predicts that light rays are deflected by gravity
- A light ray that tangentially grazes the Sun should be deflected by 1.7”
- This was confirmed in 1919 by Eddington during a total solar eclipse
- Eddington noted that under certain conditions there can be multiple light paths connecting a source and observer and hence you would get multiple images of a single source
- Lensing became interesting in 1937 when Zwicky pointed out that galaxies can split images of sources by a large enough angle to be observed
- He calculated that the probability of lensing by galaxies would be about 1% for a source at reasonably large redshift
- The first lensed quasars were observed in 1979 and the first arcs in galaxy clusters on 1986/87

Why is gravitational lensing useful?

- We can study the mass distribution of foreground matter without making dynamical assumptions about the state of that matter , e.g., velocity dispersion measurements of clusters assume that the cluster has virialized
- Lensing doesn't care whether the mass is luminous or dark as long as it interacts gravitationally
  - We can learn about the dark matter content of the universe
- The magnification of the sources in strong lensing allows us to study sources with smaller telescopes than would normally be possible
- Combining strong and weak lensing in clusters allows us to constrain both mass distribution in the cluster core as well as the halo

Abell 1689 – HST image

Cluster redshift z = 0.18
θ_E = 45″
34 multiply imaged systems
$M_{200} = 1.32 \pm 0.2 \times 10^{15}\ h^{-1}\ M_\odot$

Lensing 101 (Point-like lens)

D = angular diameter distance (ratio of an object's physical transverse size to its angular size

θ = angle of observed position of image

O = observer

β = actual angle of source wrt axis (unobservable)

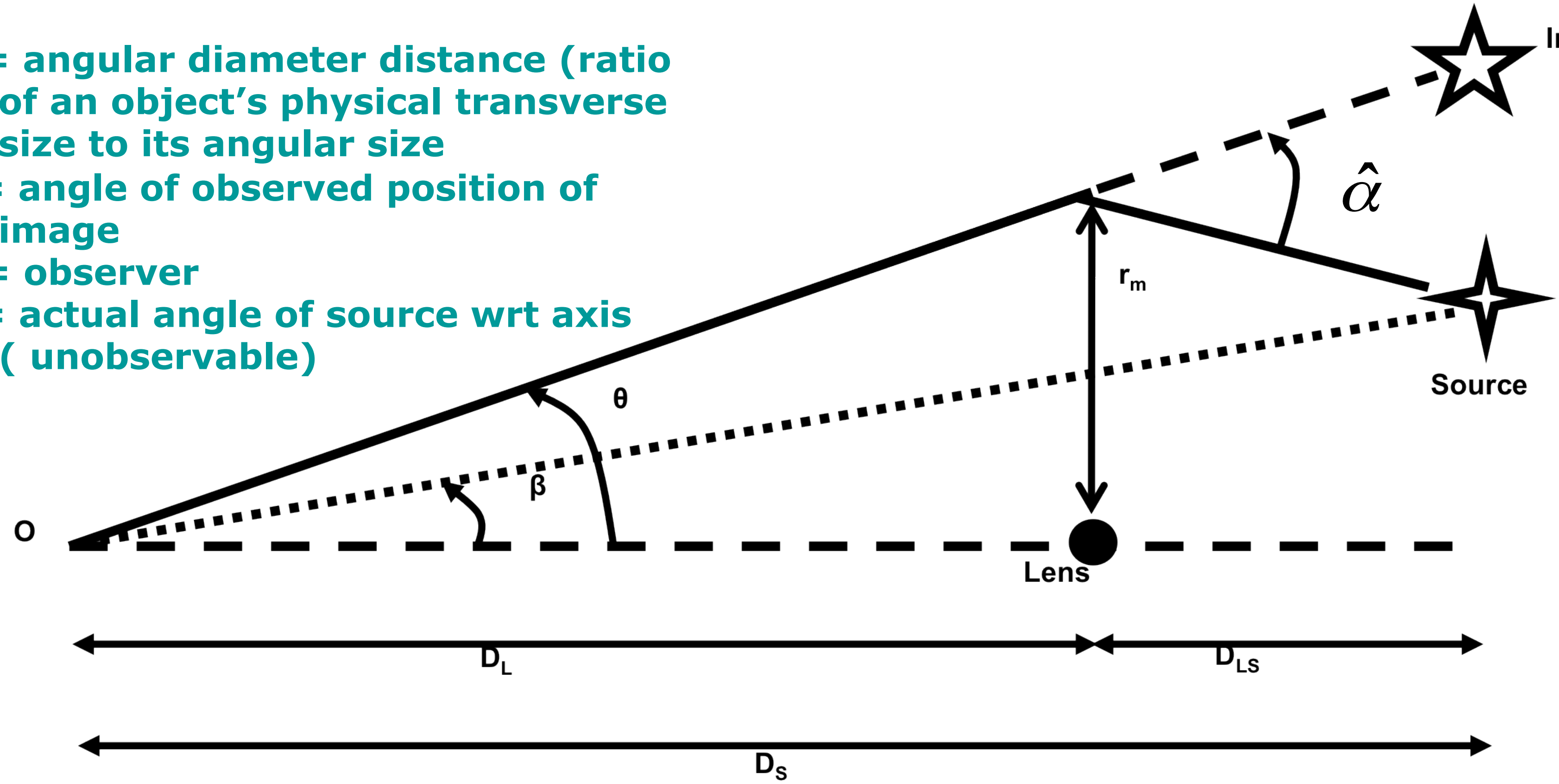

Defining angular diameter distances in this way allows us to write the lensing equation using Euclidean geometry.
Important to note that $D_s \neq D_L + D_{LS}$

Lensing Equation

- The trajectory of the light ray is bent by an angle $\hat{\alpha}$

$$\theta D_s = \beta D_s + \hat{\alpha} D_{LS}$$

- We introduce the reduced angle

$$\alpha = \hat{\alpha}\frac{D_{LS}}{D_S}, \quad \hat{\alpha} = \frac{4GM}{r_m c^2}, \quad r_m = \theta D_L, \quad \alpha = \frac{D_{LS}}{D_S D_L}\frac{4GM}{c^2\theta}$$

- So the lens equation becomes

$$\beta = \theta - \alpha$$

- This can be rewritten as

$$\theta^2 - \beta\theta - \theta_E^2 = 0, \quad \theta_E = \left(\frac{D_{LS}}{D_S D_L}\frac{4GM}{c^2}\right)^{1/2}$$

- θ_E is referred to as the Einstein angle.

Einstein Rings

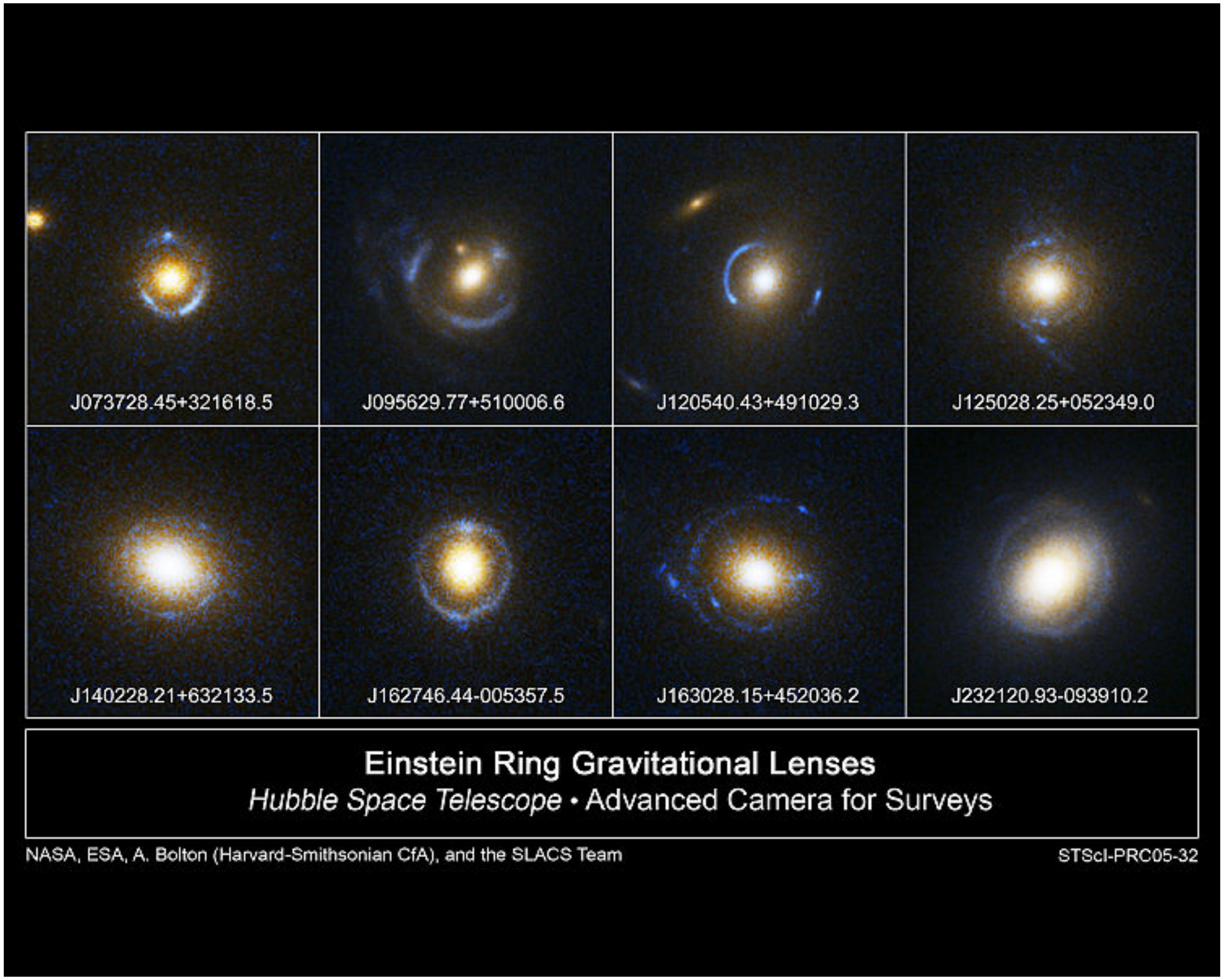

When β = 0 then the lens and the source are perfectly aligned and we get an Einstein Ring

This is fairly rare

Extended lenses

- In reality the lens is an extended object such as a galaxy or a cluster
- In this case the lens equation becomes vectorial

$$\vec{\beta} = \vec{\theta} - \vec{\alpha}, \quad \vec{\alpha} = \frac{\vec{\hat{\alpha}} D_{LS}}{D_S}, \quad \vec{\theta} = \frac{\vec{\xi}}{D_L}$$

- ξ is the two dimensional vector indicating the position in the lens plane
- After some substitutions we can write the lens equation as

$$\vec{\beta} = \vec{\theta} - \vec{\nabla}_{\theta} \Psi\left(\vec{\theta}\right)$$

- This equation in non-linear in $\vec{\theta}$ so for some source positions there may be multiple solutions of the lens equation. This corresponds to the formation of multiple images in the so-called strong lensing regime

Source Magnification

- The surface brightness of the source is not changed by the deflection of light due to gravity
- However the source shape becomes distorted
- This leads to amplification of the source brightness

$$A = \frac{d\Omega}{d\Omega_0}$$

Observed solid angle

Actual solid angle in the absence of the lens

- We can define a mapping matrix *T* that relates the angles β and θ

$$T = \begin{pmatrix} 1-\kappa-\gamma_1 & -\gamma_2 \\ -\gamma_2 & 1-\kappa+\gamma_1 \end{pmatrix}$$

Source Magnification

- κ is called the convergence. It changes the of the source but not the shape

$$\kappa(\theta) = \Sigma(\theta)/\Sigma_{cr}, \quad \Sigma_{cr} = \frac{c^2 D_S}{4\pi G D_L D_{LS}}$$

- Σ(θ) is the surface mass density
- γ is the shear. It distorts the shape of the object

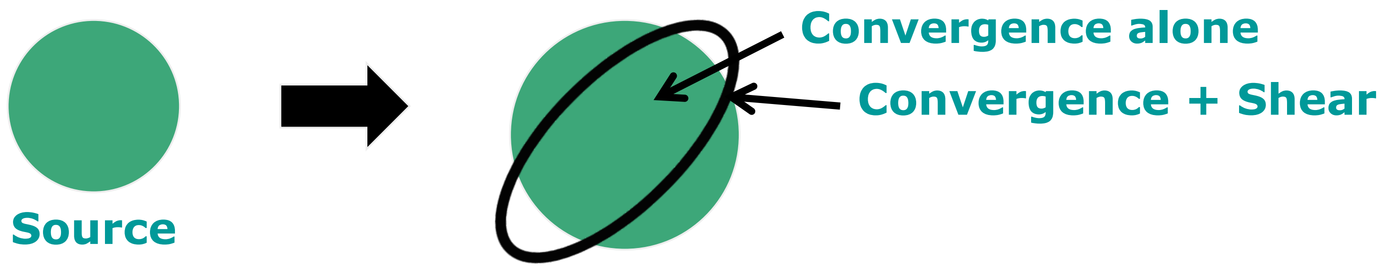

- The magnification is written as

$$A = \det\left(T^{-1}\right) = \frac{1}{(1-\kappa)^2 - \gamma^2}, \quad \gamma^2 = \left(\gamma_1^2 + \gamma_2^2\right)^2$$

- To get multiple images requires κ(θ) > 1 - γ

Caustics and Critical Lines

- The magnification of the source can be infinite for certain source positions (only strictly true for point sources)
- These locations are known as caustics.
- The images of these caustics are known as the critical lines – the directions in the image plane along which a source would be infinitely magnified.
- When a source crosses a caustic images appear and disappear in pairs.
- The total number of images produced by a transparent lens is always odd – Burke's theorem
- This is true for non-singular lenses but does not always hold for singular ones.
- For lenses with multiple images at least one of the images has negative parity, meaning its image is inverted

Some elliptical lens topologies

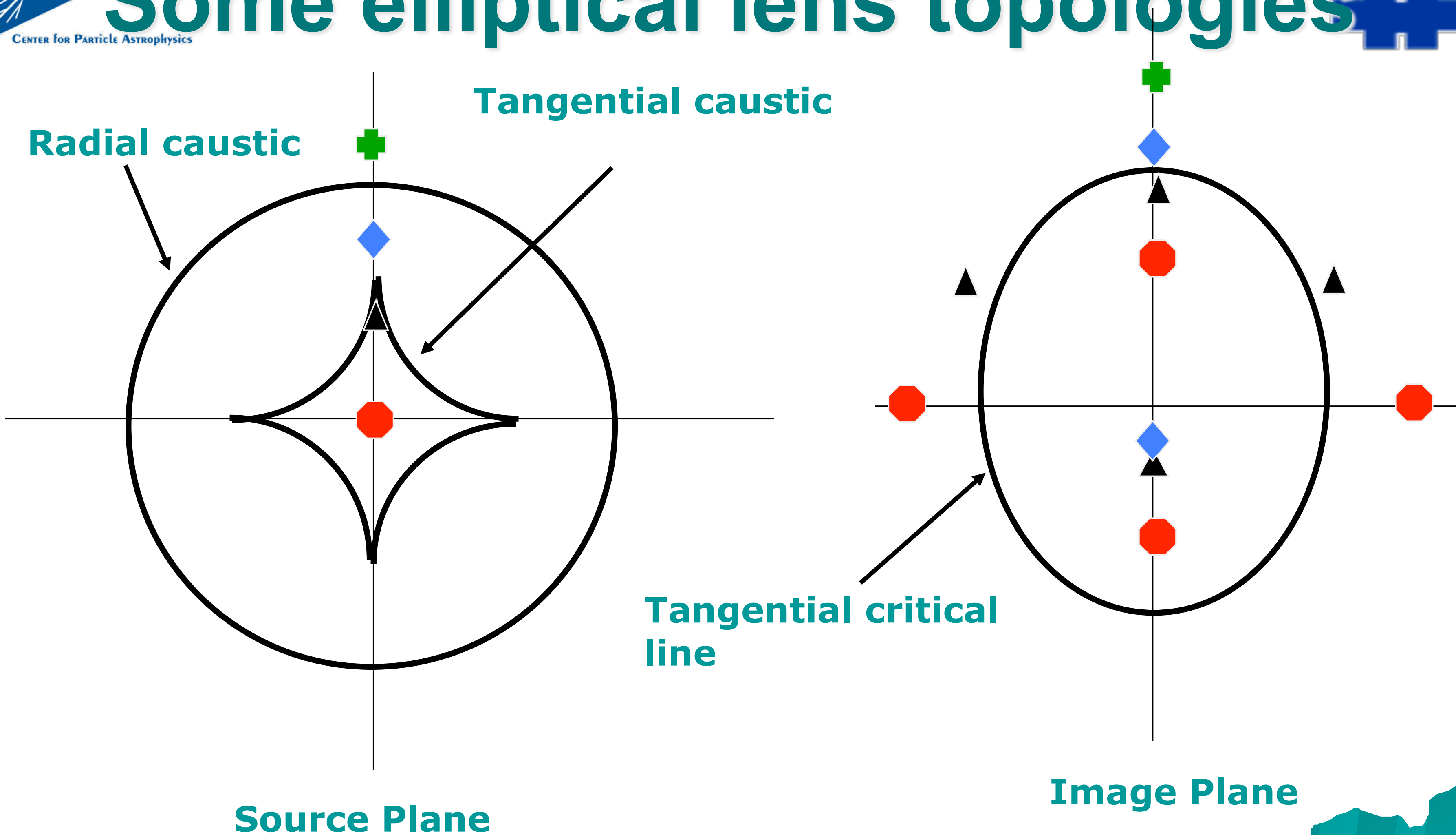

Weak Lensing in Clusters

- If the density of the cluster is less than Σ_{crit} or we look in regions outside the giant arcs where $\kappa < 1 - \gamma$ where there are no multiple images then we are in the weak lensing regime.
- It is not easy to measure κ because it is typically much less than one
- However the images are magnified by a factor $A_1 = (1 - \kappa + \gamma)^{-1}$ in one direction and $A_2 = (1 - \kappa - \gamma)^{-1}$ in the orthogonal one. So the shear induces tangential distortions of the images.
- A circular source will be deformed into an ellipse with axis ratio $r = A_1/A_2$ so the average ellipticity is

$$\langle \varepsilon \rangle = (1 - r)/(1 + r) = \gamma / (1 - \kappa)$$

- When $\kappa \ll 1$ the average ellipticity gives directly the shear

Weak Lensing in clusters

No lensing, galaxies oriented randomly

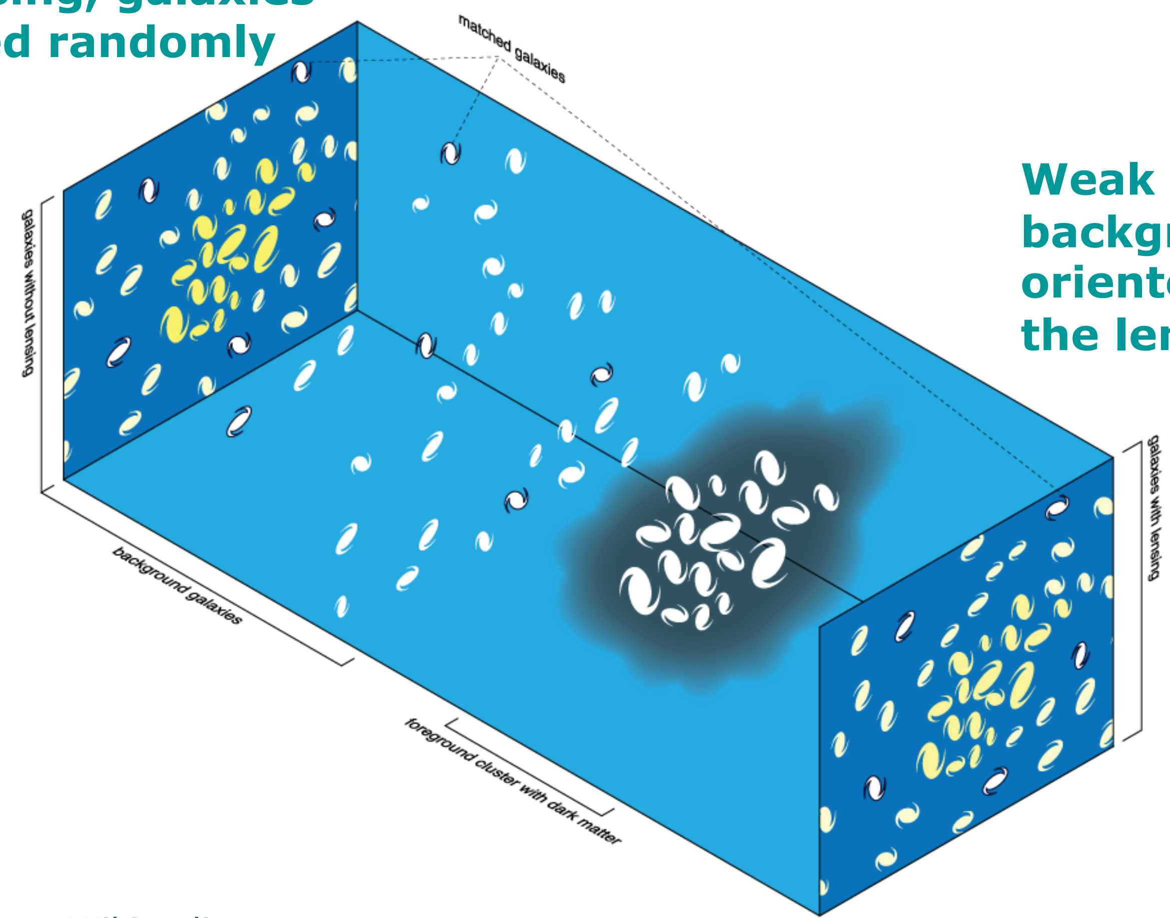

Weak lensing, the background galaxies are oriented tangentially to the lens and stretched.

Image from Wikipedia.
Author Michael Sachs

Weak lensing issues

- The source galaxies have intrinsic ellipticity, referred to as shape noise
- The PSF can have an elliptical component, referred to as the PSF anisotropy, typically 1-10% depending on the telescope
- PSF broadening due to seeing reduces the signal for source galaxies that are not much large than the PSF
- Mass sheet degeneracy. In the absence of magnification information the convergence can only be determined up to a transformation $\kappa \to \kappa' = \lambda\kappa + (1-\lambda)$ where λ is an arbitrary constant
- Angular resolution is limited by the source density, number of galaxies per arcmin^2
- Knowledge of the source redshift distribution

Sloan Digital Sky Survey

- SDSS-I imaged more than 8,000 square degrees of the sky in five optical bandpasses, and it obtained spectra of galaxies and quasars selected from 5,700 square degrees of that imaging. It also obtained repeated imaging (roughly 30 scans) of a 300 square degree stripe in the southern Galactic cap (Stripe 82)
- SDSS-II completed the original SDSS imaging and spectroscopic goals. The final dataset includes 230 million celestial objects detected in 8,400 square degrees of imaging and spectra of 930,000 galaxies, 120,000 quasars, and 225,000 stars.

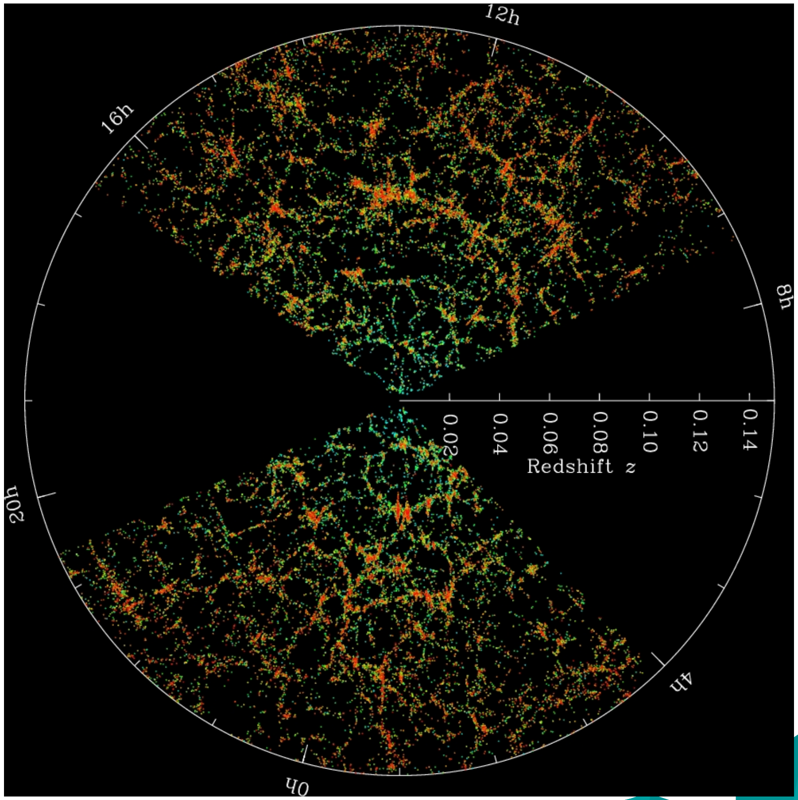

How did we get into strong lensing

- **8 o'clock arc (Allam et al. 2007)**
  - Discovered serendipitously in inspection of SDSS DR4 interacting galaxy pairs sample
  - z = 2.73 Lyman Break Galaxy (LBG) lensed by z = 0.38 SDSS luminous red galaxy (LRG)
  - Bright, blue arc (total r = 19), ~4" away from LRG
  - Easy absorption line redshift in 20 min DIS spectrum on APO 3.5m

- **cB58 (Yee et al. 1996)**
  - Discovered serendipitously in CNOC1 cluster redshift survey
  - z = 2.72 LBG lensed by z = 0.37 brightest cluster galaxy (BCG)
  - Bright, blue object (r = 20.4), 6" away from BCG
  - Bright enough to be easily seen in SDSS and to have an SDSS spectroscopic redshift!

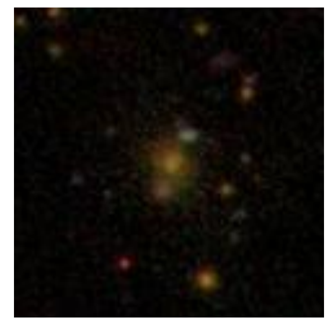

- **Start *systematic search* for more systems like cB58 and the 8 o'clock arc in the SDSS**

8 o'clock arc

Allam et al., 2007, ApJ 662, L51

APO 3.5m g-band image and Keck LRIS spectrum

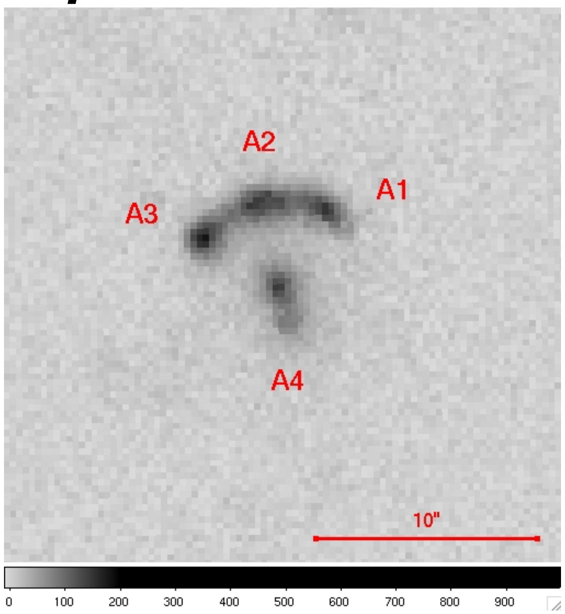

z_{lens} = 0.38

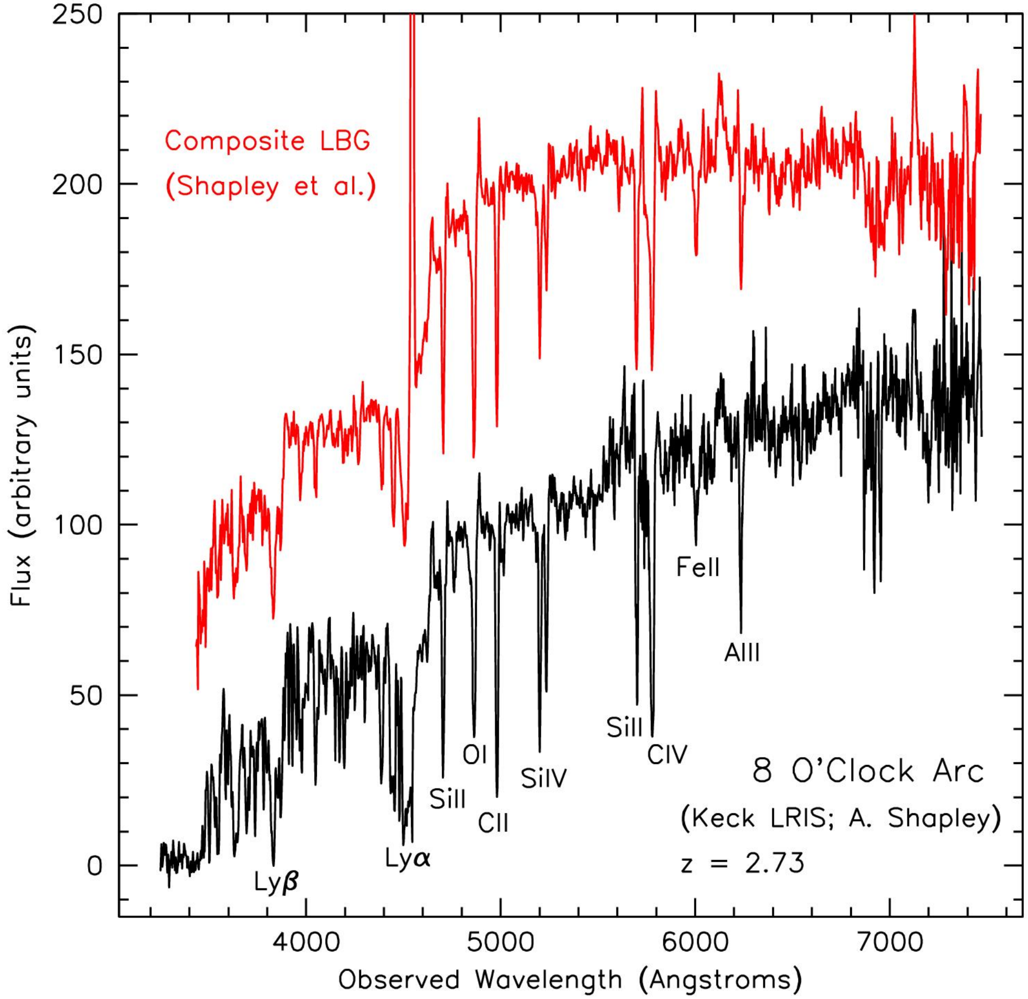

SDSS Arc Search

- The candidates come from two different samples.
  - Potential red galaxy lenses from SDSS DR5 (8000 deg^2)
    - 221,000 luminous red galaxies (LRGs)
    - 29,000 brightest cluster galaxies (BCGs) from maxBCG cluster sample (J. Annis)
    - SDSS DR5 CAS database query (D. Kubik – Masters Thesis)
      - Blue galaxies (g-r < 1 and r-I < 1 color cuts)
      - < 10" from LRG or BCG
      - 57,000 systems returned with n=1 or more blue objects
      - Rank systems by number of blue objects n
    - Visual inspections
      - Inspect all systems (1081) with n ≥ 3 blue objects
      - 4 separate inspectors looked at SDSS CAS gri color jpeg images
      - Follow up 14 candidate systems flagged by 2 or more inspectors
      - Plus 1 more ("clone") from single-inspector eye scan of n=2 LRG list
  - Interacting-merging galaxy sample (S.Allam)
    - Start with 15,000 isolated galaxies and 38,000 isolated galaxy pairs from SDSS DR5
    - Exclude spiral galaxies to avoid false detections of lenses
    - Apply additional selection cuts.
    - Yields 17500 objects which after visual examination reduces to 3000 potential objects – too many to observe!

Follow-up Observations

- The SDSS search identified 14 candidate systems. We have also selected promising candidates from the Allam sample.
- Follow-up observing program (Fermilab group) on Apache Point Observatory (APO) 3.5m telescope
  - Arcs are bright (r ~ 20-22) and high SB (μ_r ~ 23-24 mag/arcsec^2)
  - SPIcam gri imaging (15 min exposures per filter) for deeper images (SDSS discovery images are only 54 seconds on a 2.5m telescope)
  - DIS spectroscopy (45 min exposures) of brighter targets for source and lens redshifts. Some of our newer targets take several hours
- We curently have 16 spectroscopically confirmed lensing systems.
  - 9 with $z \geq 2$ (one is at 1.82)
  - 7 have z ~1.0
  - Lenses typically have z ~ 0.4
- Other follow-up data
  - HST data for 13 systems. Have submitted a Cycle 18 proposal for 9 objects
  - Imaging data from the WIYN telescope on Kitt Peak
  - Spectroscopy from the Mayall telescope on Kitt Peak
  - Spitzer data for two systems (lrg-2-2811 and bcg-3-817)
  - Gemini NIRI spectroscopy of 3 confirmed z > 2 systems
  - IRAM mm CO and continuum observations of z > 2 systems
  - IRTF near-IR imaging follow-up

9 Spectroscopically Confirmed Lensing Systems (1’ x 1’)

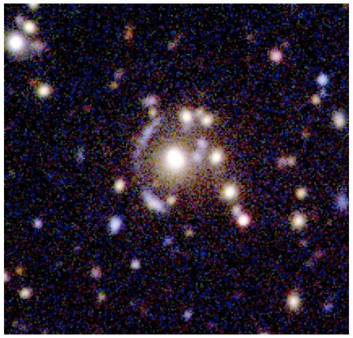

lrg-3-817
$z_l = 0.35$
$z_s = 2.26$

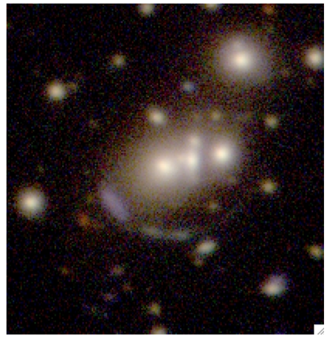

SSA_1113
$z_l = 0.35$
$z_s = 0.77$

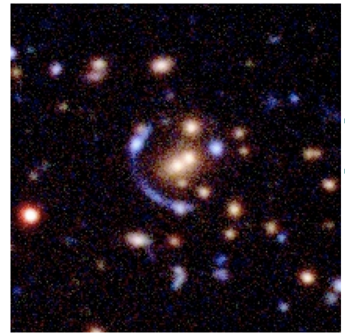

lrg-4-606
$z_l=0.49$
$z_s = 2.03$

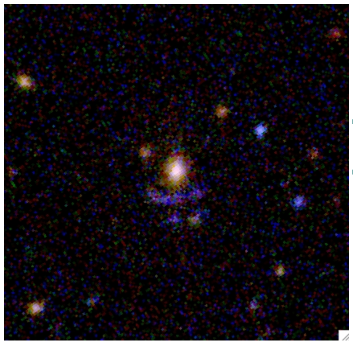

lrg-3-227
$z_l = 0.45$
$z_s = 0.98$

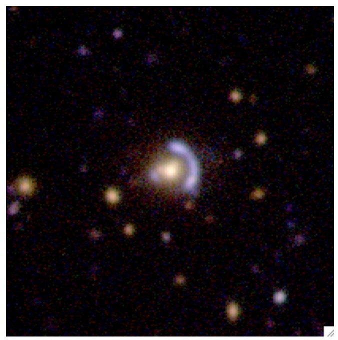

lrg-2-2811
$z_l = 0.42$
$z_s = 2.0$
“The Clone”

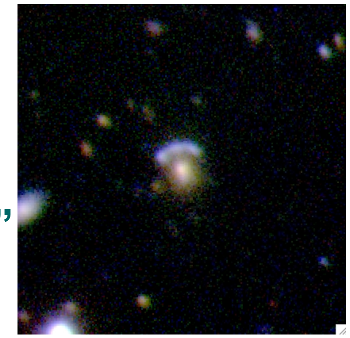

8 o’clock arc
$z_l = 0.38$
$z_s = 2.73$

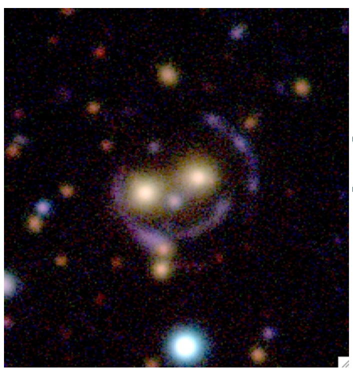

lrg-4-581
$z_l = 0.43$
$z_s = 0.97$
“Cosmic Snowman”

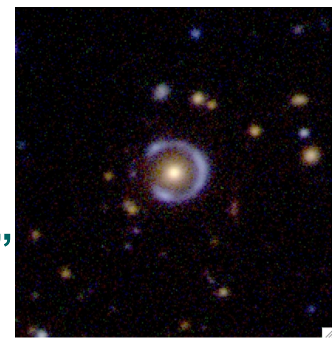

lrg-3-757
$z_l = 0.44$
$z_s = 2.38$
“Cosmic Horseshoe”

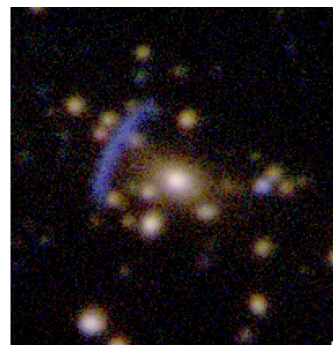

SSA_1343
$z_l = 0.34$
$z_s = 2.1$

7 further systems

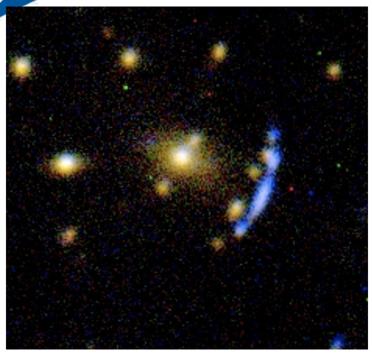

8004
z_l = ~0.5
z_s = 1.82

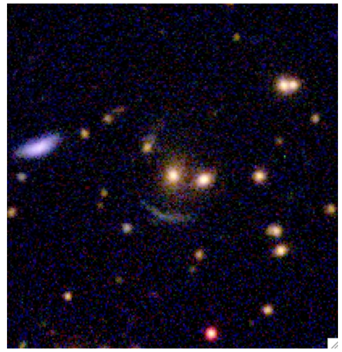

bcg_3_067
z_l = 0.355
z_s = 2.2 ?

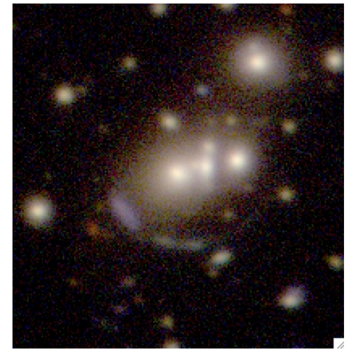

1113
z_l = 0.34
z_s = 0.77

100173
z_l = 0.48
z_s = 2.94

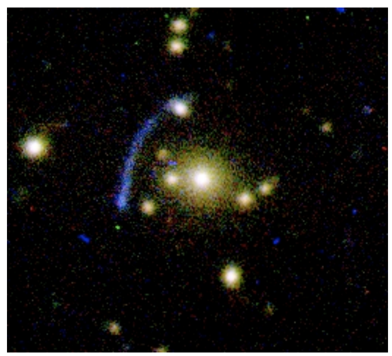

1154
z_l = 0.42
z_s = ?

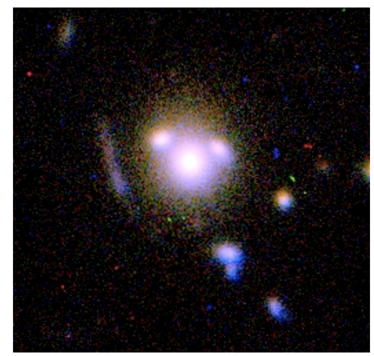

5185
z_l = 0.25
z_s = 0.66

lrg_4_670
z_l = 0.41
z_s = ?

HST Images

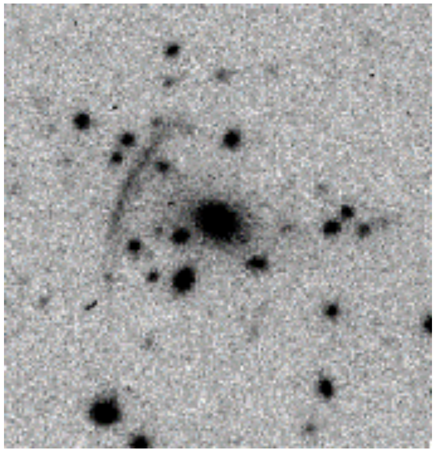

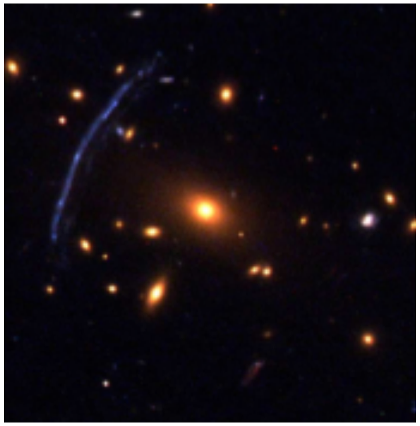

SSA_1343
z = 2.09

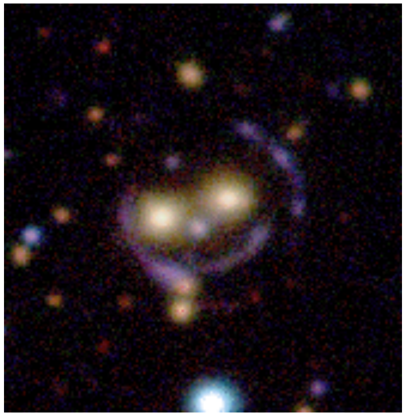

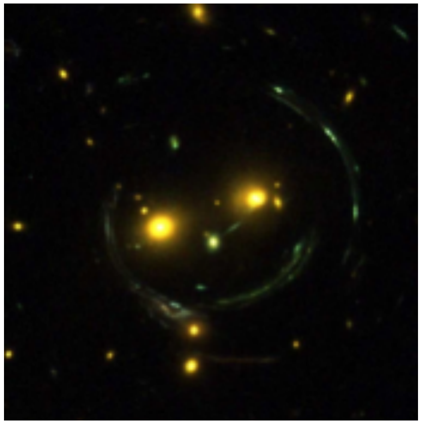

lrg-4-581
z = 0.97

lrg_2_2811 ("Clone")

Lin et al., 2009, APJ 699 1242

Subaru FOCAS V-band image and spectrum (M. Oguri)

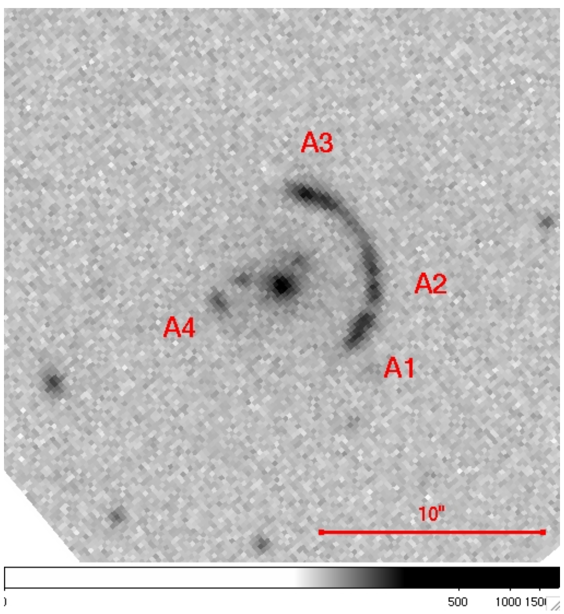

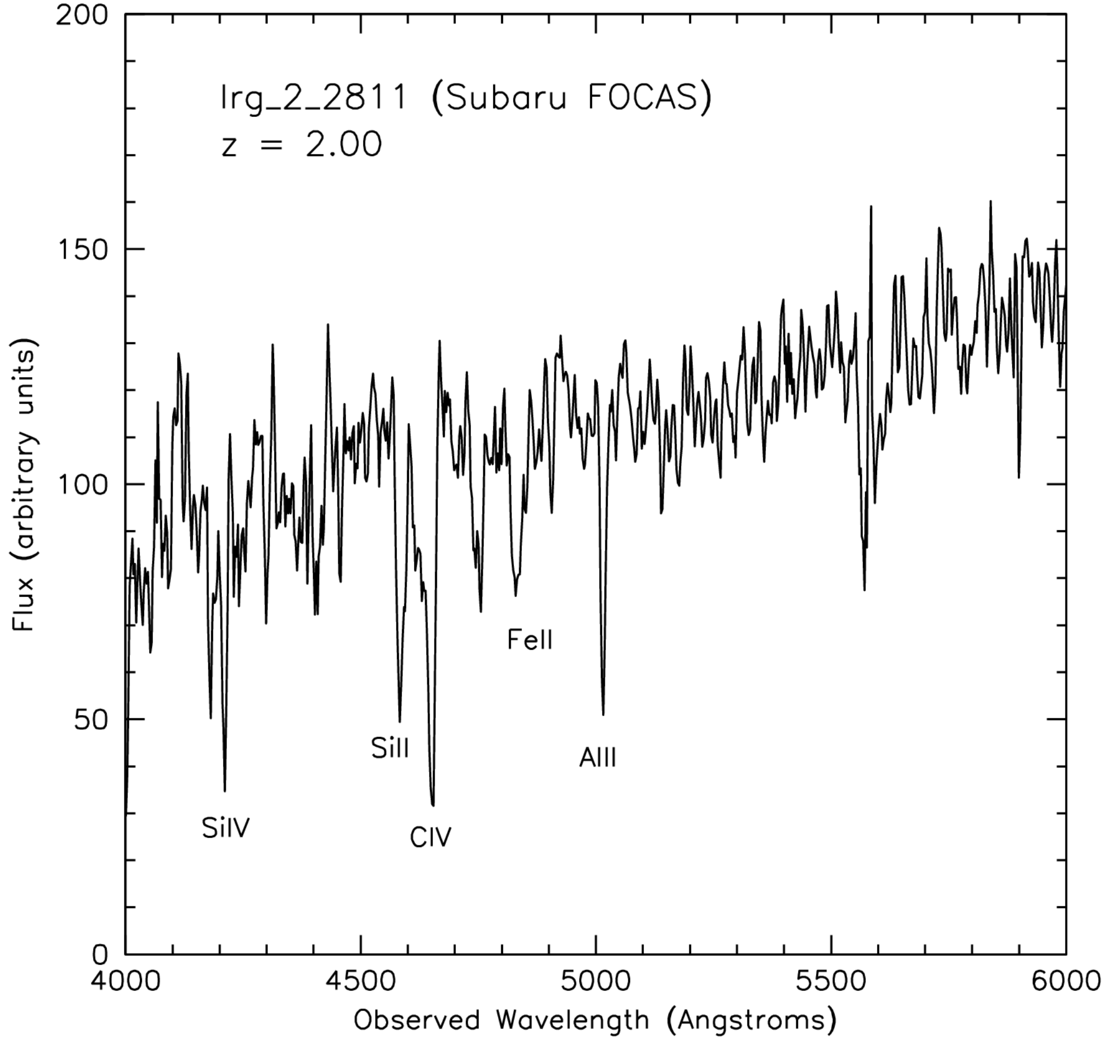

z_{lens} = 0.42

Comparison of SDSS, Subaru and HST Data for lrg-2-2811

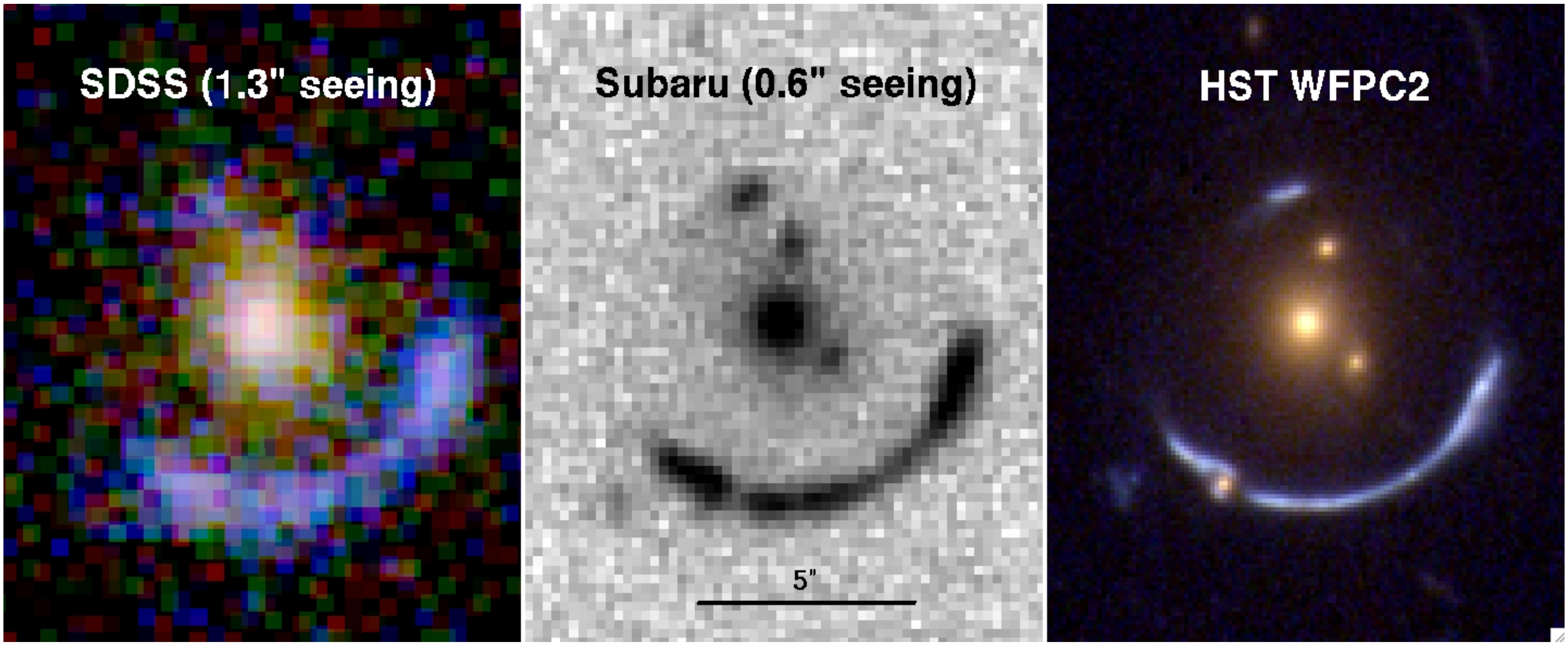

Lens Modeling

- Use lensmodel/gravlens (C. Keeton, astro-ph/0102340)
  - Uses x,y positions of images
  - Image positions and fluxes are derived from running Sextractor on the images after subtraction of the rest of the objects in the field (using GALFIT Peng et al. 2008, AJ 124, 266).
  - Has a wide variety of mass models
  - Works best when there are well defined bright knots in the source that can be identified.
- LENSVIEW (R. Wayth & R.L. Webster, MNRAS 372 (2006) 1187-1207).
  - Uses the full FITS image along with an input PSF and a noise image. The other objects in the images are subtracted.
  - Generates a model image, convolves it with the PSF and compares to the input image
  - Provides a prediction for the un-lensed source in the form of a FITS image
  - Good for situations when the source does not have well defined bright regions
  - Has a rather limited set of mass models
  - Hard to accommodate flux anomalies in the model

Modeling Results for 8 o'clock arc

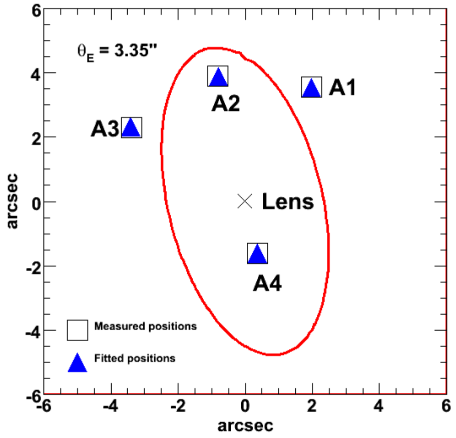

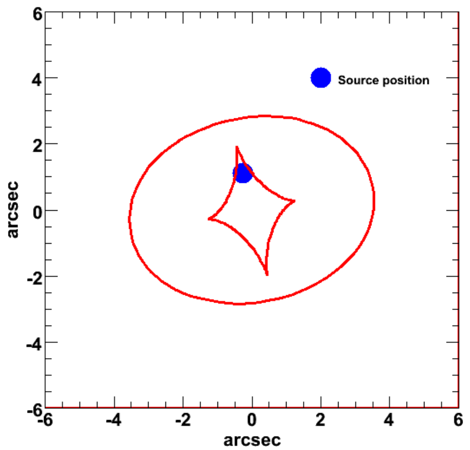

Fit a Singular Isothermal Ellipse
θ_{EIN} = 3.35"
ε = 0.53
PA = 12.8 deg
χ^2/dof = 1.04
σ = 392 km s^{-1}
R_{EIN} = 12.2 h^{-1} kpc
M_{EIN} = 1.4 x 10^{12} h^{-1} $M_\odot$
M/L (rest frame g-band) = 13.8 h $M_\odot$ /$L_\odot$
Total Magnification = 12.8

Lens Modeling Results for lrg-2-2811- 'The Clone'

- Using Subaru data and the LENSVIEW code
- Assume a Singular Isothermal Ellipse (SIE) mass profile

$$\Sigma(\xi) = \frac{\sqrt{f}\sigma^2}{2G} \frac{1}{\sqrt{\xi_1^2 + f^2 \xi_2^2}}, \quad \sigma^2 = \frac{\theta_E c^2 D_S}{4\pi D_{LS}}$$

- ξ is the radial coordinate and f is the axis ratio, σ is the velocity dispersion
- Flat cosmology, Ω_m=0.3, Ω_Λ=0.7, H_0=100 h km s^{-1} Mpc^{-1}
- Fit for the Einstein radius θ_{EIN}

Lens Modeling Results for lrg-2-2811- 'The Clone'

Model Image

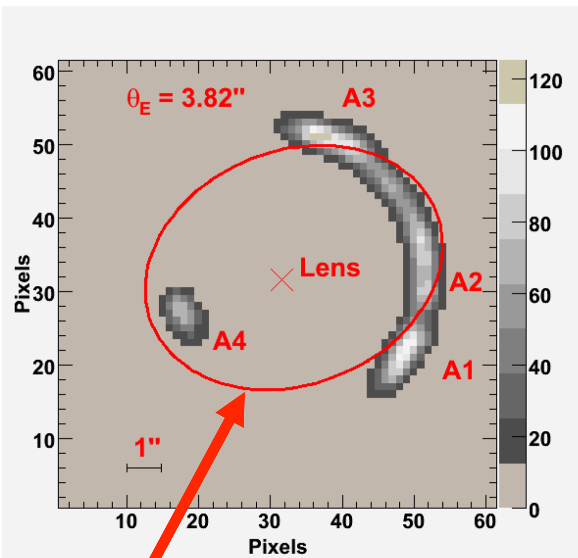

Source

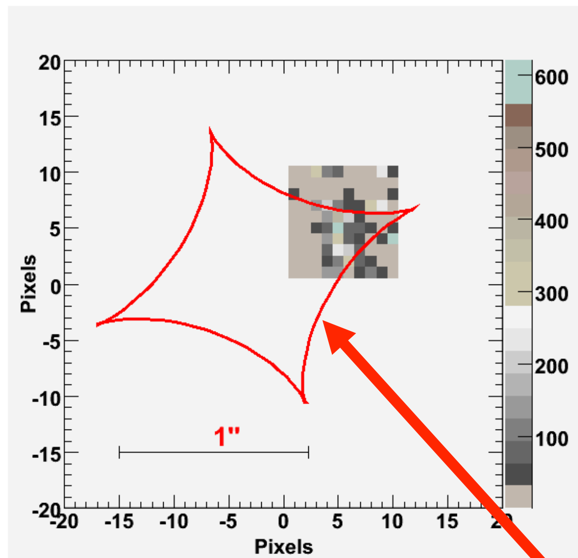

Residuals

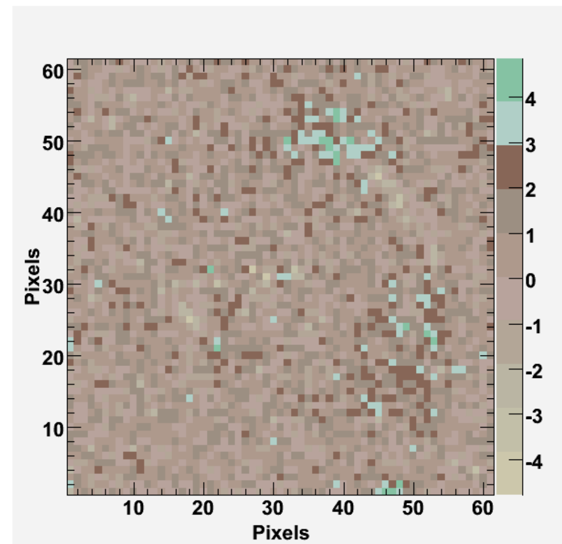

Tangential Critical curve

Tangential caustic

χ^2 = 2.18, θ_E = 3.82± 0.03", σ = 440±7 km s^{-1}

Magnification = 27±1, M(< θ_E) = 2.1±0.3 × 10^{12} $h^{-1}M_{\odot}$

Analysis of the model

- Notice that the χ^2 is not very good. Most of the discrepancy comes from knot A3 which is brighter in the data than in the model
- It has been known for some years that smooth mass models such as the SIE fit the image positions well but not always the fluxes. This has been explored in the literature, e.g Keeton et al 2005, ApJ 635, 35
- With LENSVIEW it is not possible to decouple the images positions from the flux as the whole image is modeled
- In lensmodel we can increase the errors on the fluxes to de-weight them in the χ^2 . We get a χ^2/dof of 0.85
- The parameters of the lensmodel fit agree well with those from LENSVIEW

Flux anomalies

- The lens lrg-2-2811 is a "fold" configuration lens

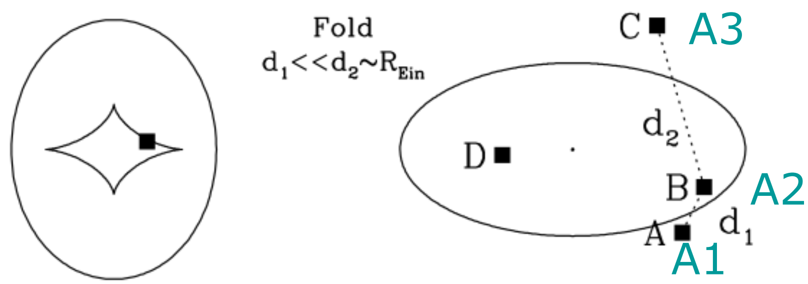

- We define the ratio $R_{fold} = (F_+ - F_-)/(F_+ + F_-)$ where F_+ and F_- are the fluxes for a pair of images of opposite parity. We measure R_{fold} = 0.173 for the image pair A3-A2

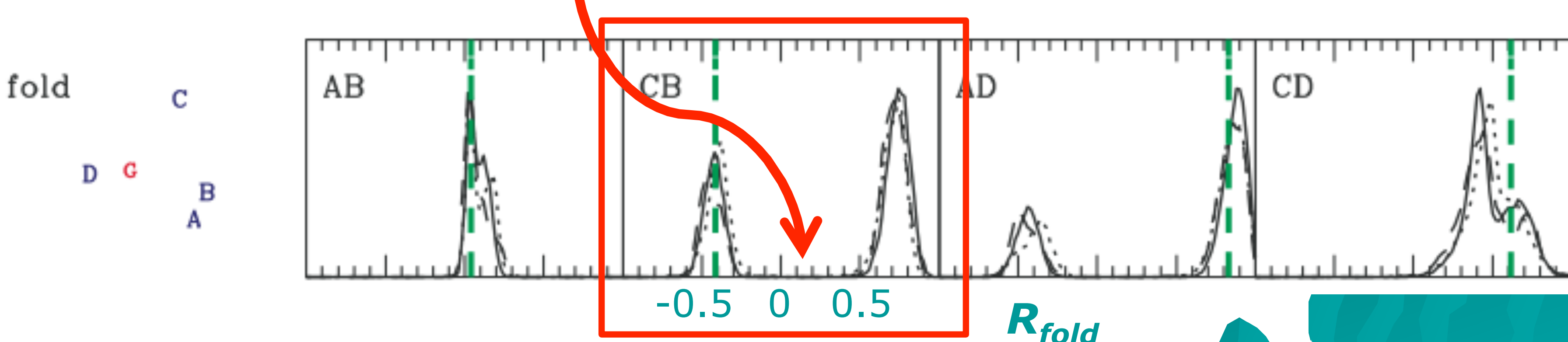

lrg_4_606

Diehl et al., 2009, ApJ 702 L110

APO 3.5m SPIcam gri image and DIS spectrum (unfluxed) HST images due March 13

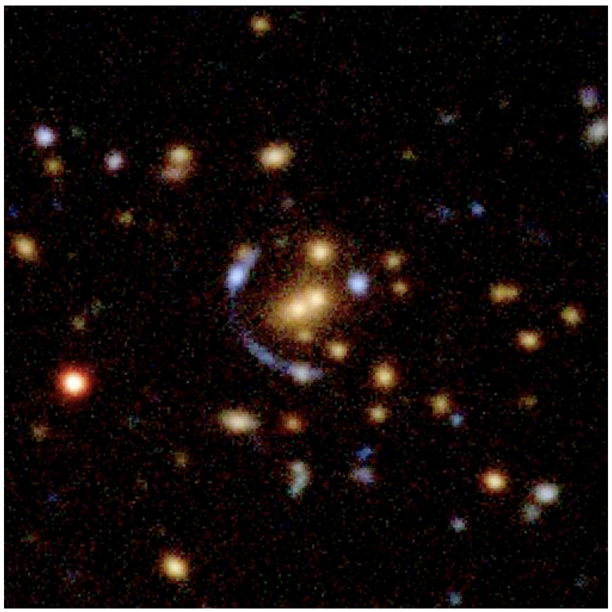

$z_{lens} = 0.49$

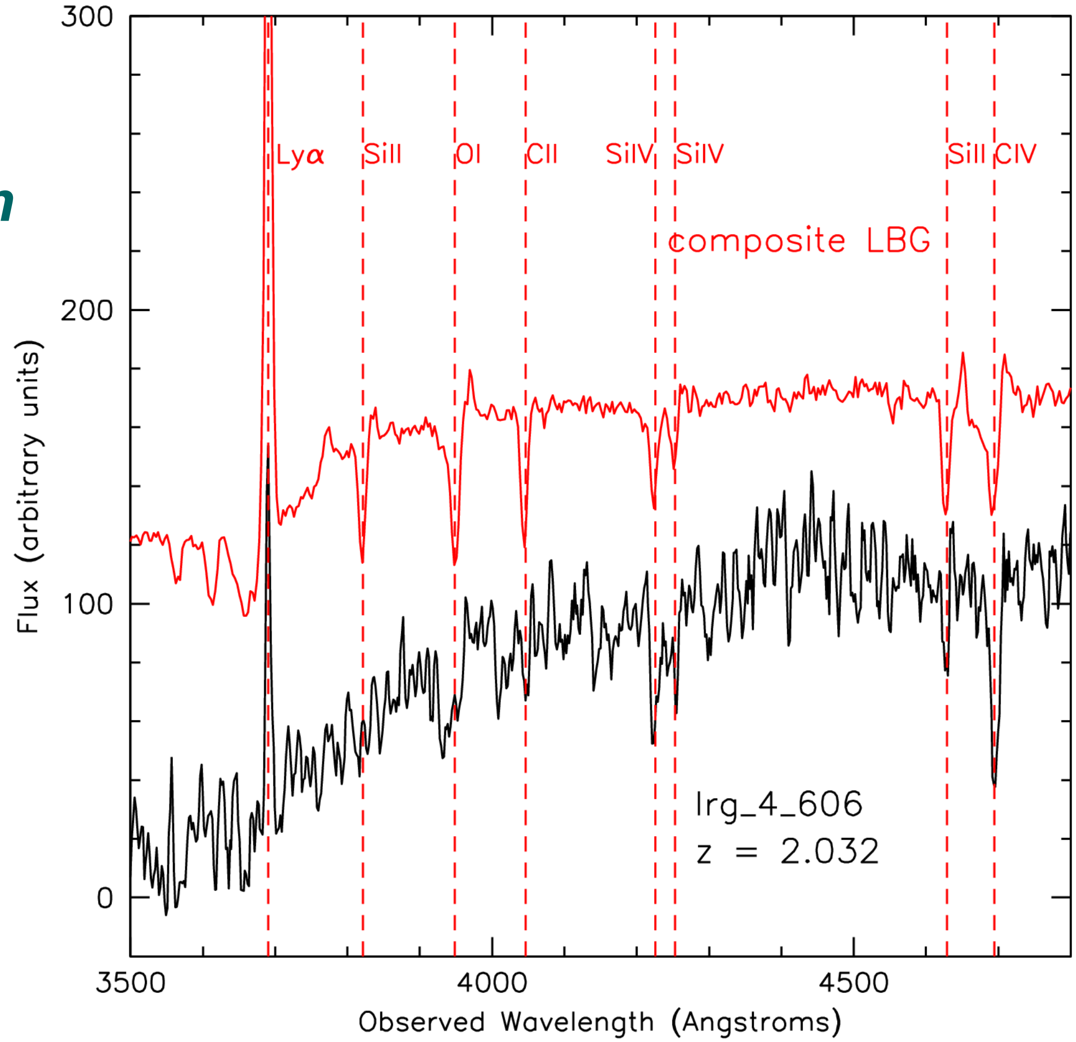

Modeling for lrg-4-606

- An example of using GALFIT to model the light profiles of the galaxies and the arcs

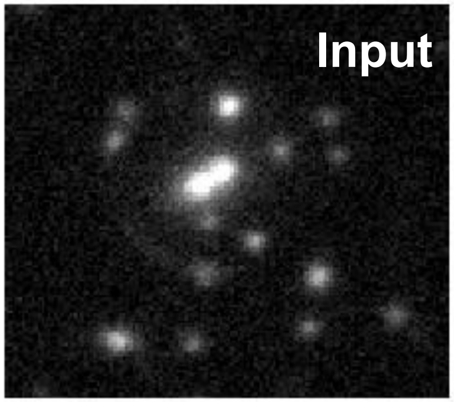

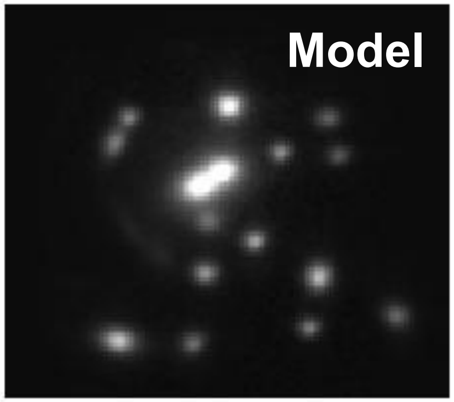

i band

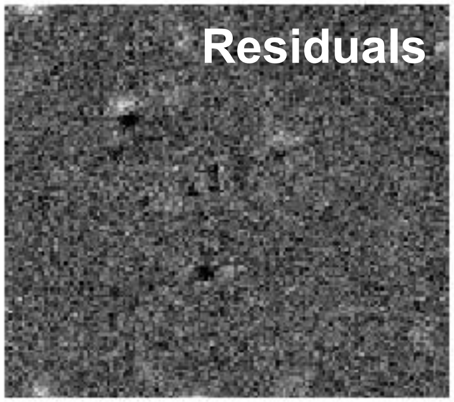

Combination of Sersic profiles for the galaxies and exponential disks for the arcs
18 objects + sky
χ^2/dof = 1.4

Modeling results for lrg-4-606

Model

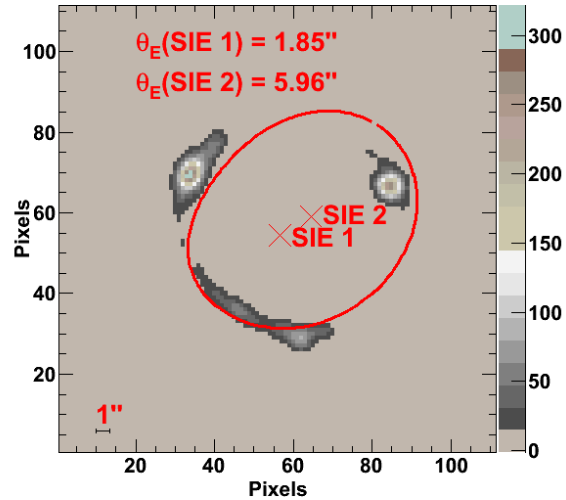

Source

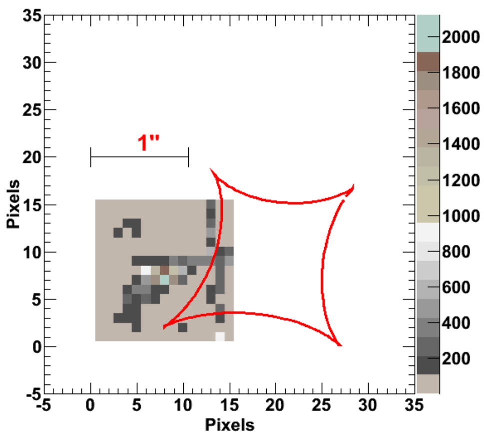

Residuals

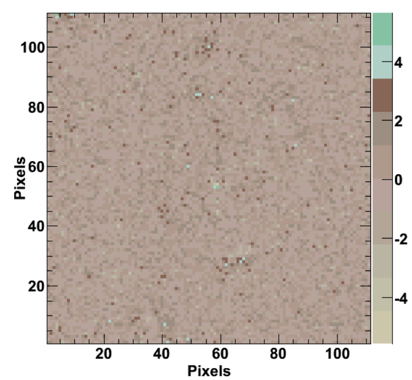

Uses LENSVIEW
χ^2/dof = 1.13
Model uses two Singular Isothermal Ellipses centered at the position of the two central galaxies
This type of model has been used successfully on other systems with binary galaxies

$M(< \theta_E) = 11.6 \pm 2.7 \times 10^{12}\ M_\odot$

lrg_3_817

Diehl et al., 2009, ApJ 702 L110

APO 3.5m SPIcam gri image and DIS spectrum (unfluxed)

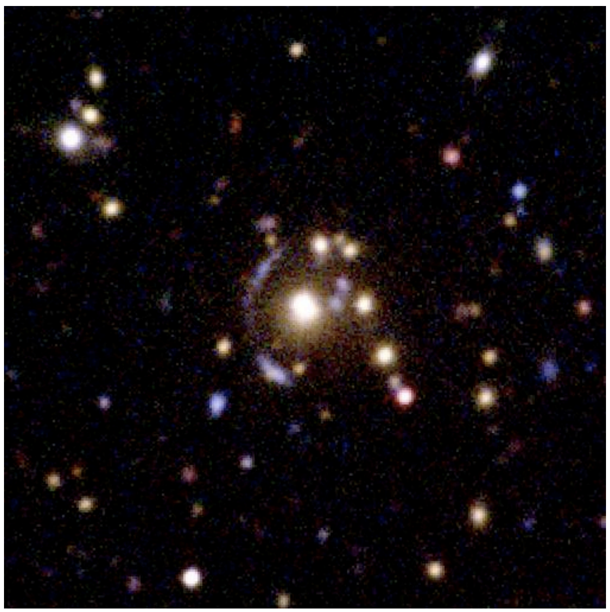

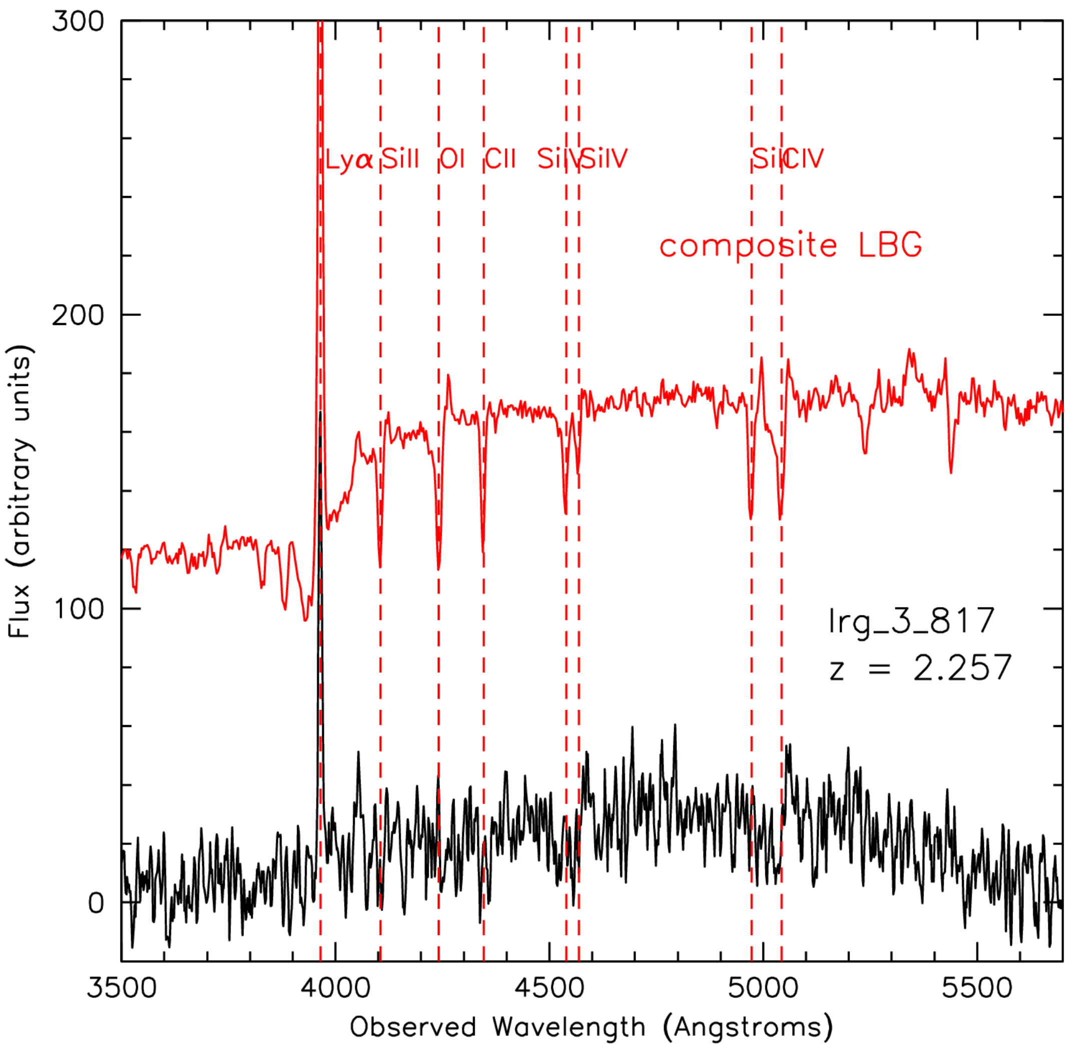

z_{lens}= 0.35

March 4 2010

Modeling results for lrg-3-817

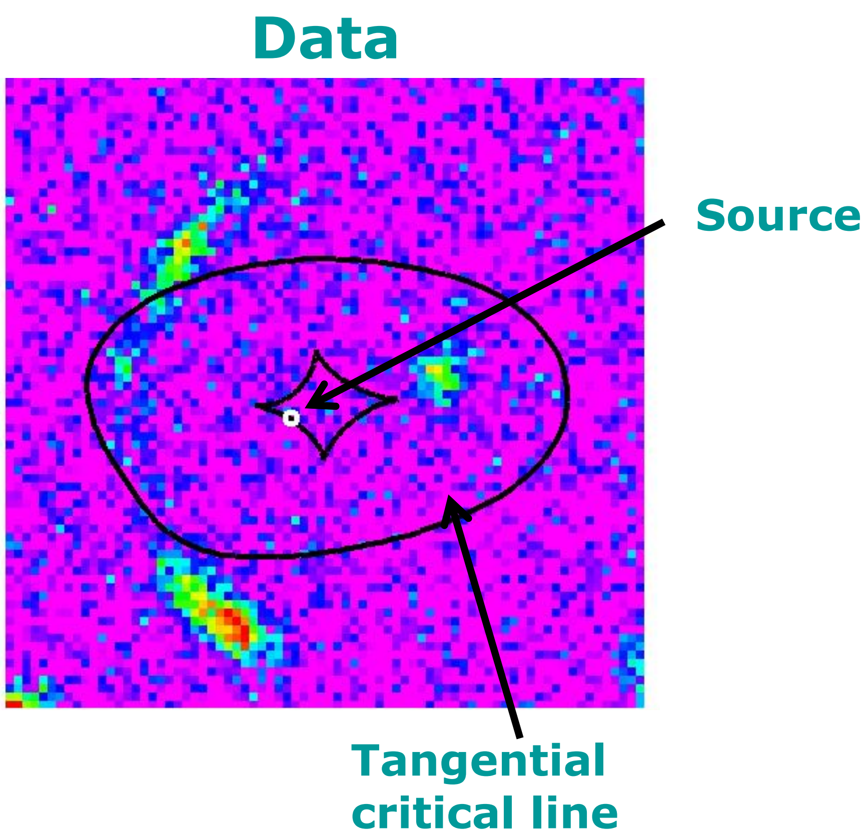

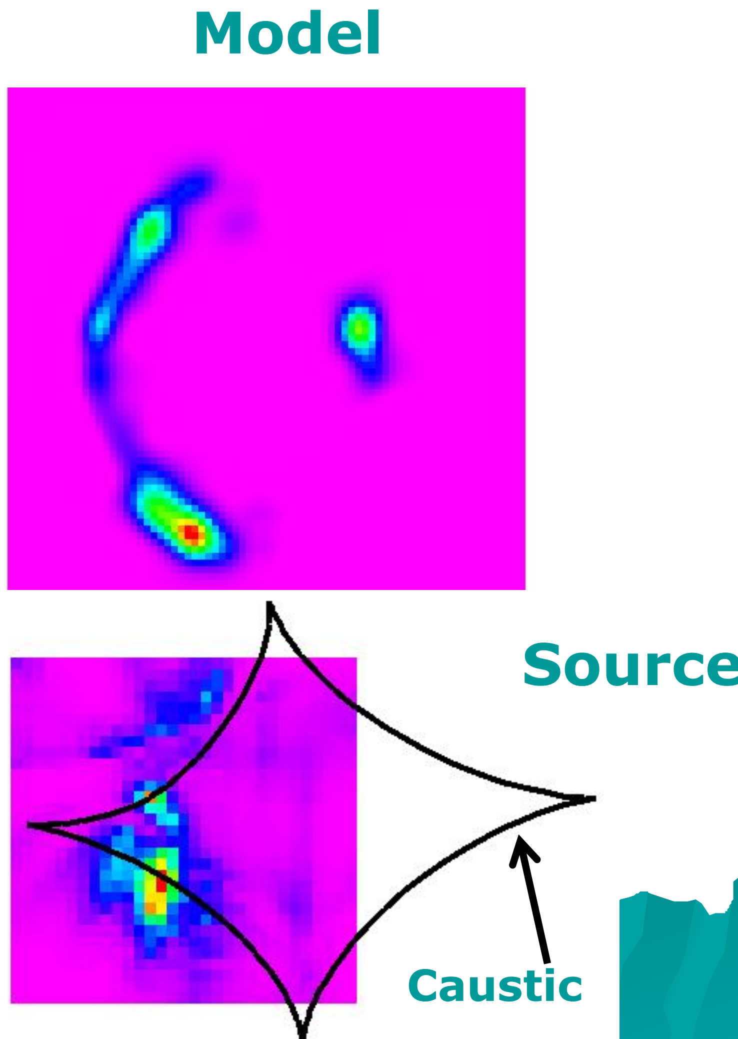

$\theta_E = 7.7 \pm 1.1''$
$M(< \theta_E) = 9.6 \pm 2.7 \times 10^{12}\ M_\odot$
(work of Anderson West, IMSA student)

Blanco Cosmology Survey (BCS)

- A 60 night NOAO imaging survey program from 2005 until 2008 using the MOSAIC II camera on the Blanco 4m at CTIO (Southern Hemisphere)
- 75 deg^2 of sky in SDSS *griz* bands
- Overlaps with South Pole Telescope area
- Two fields near $\delta = -55°$, one at $\alpha = 23.5$ hr and the other at $\alpha = 5.5$ hr.

Roger Smith/NOAO/AURA/NSF

Elliot Arc

- During the Fall 2006 observing for BCS at CTIO I serendipitously discovered a strong lens while looking at the images we were taking – you have to do something to stay awake at 3am!
- As I discovered I got to name it. Called it the "Elliot Arc" after my 8 year old nephew – who was very excited by the prospect!

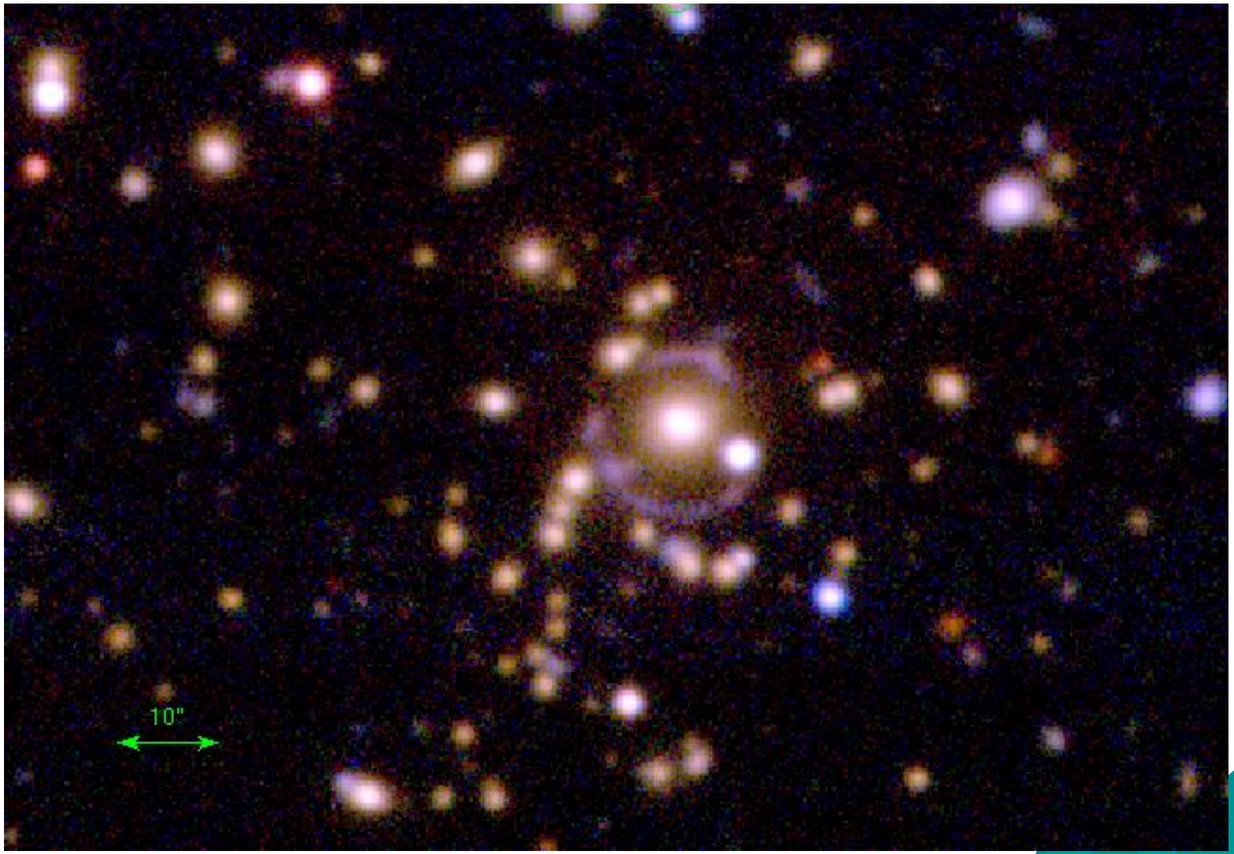

Spectroscopic Follow-up

- **Obtained Gemini GMOS multi-object spectroscopy in August 2007. We targeted the 4 knots labeled as well as 51 additional objects.**

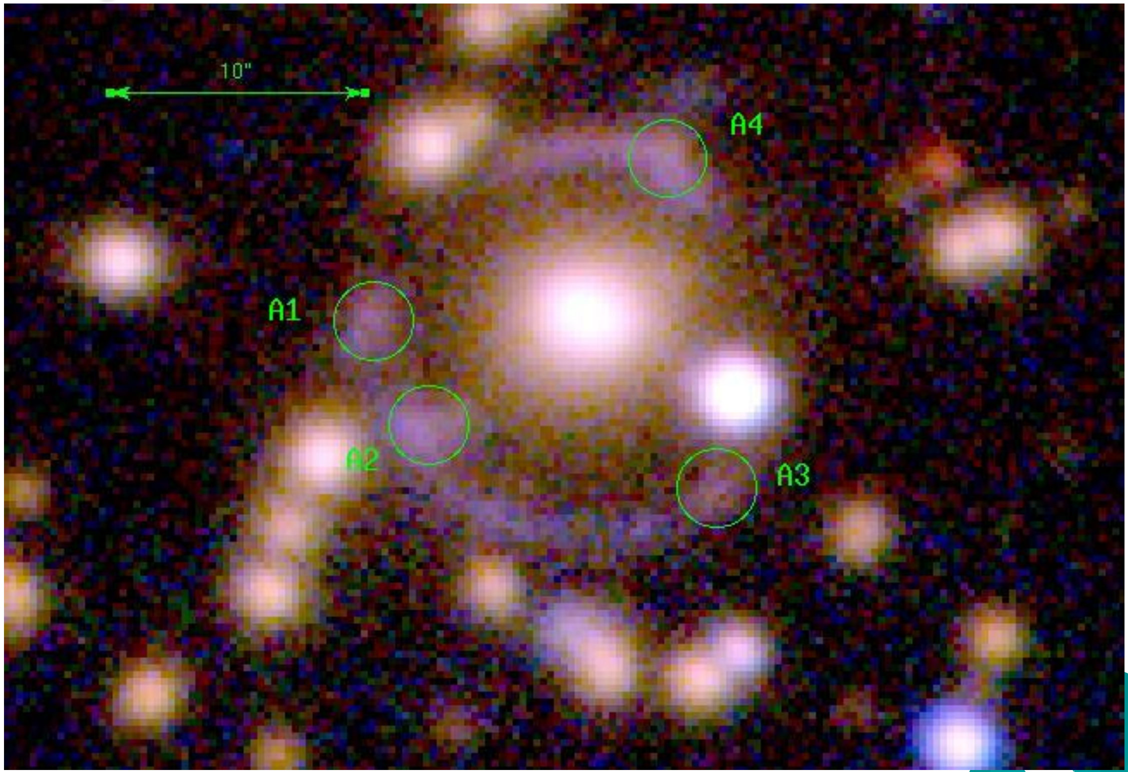

Elliot Arc Spectra

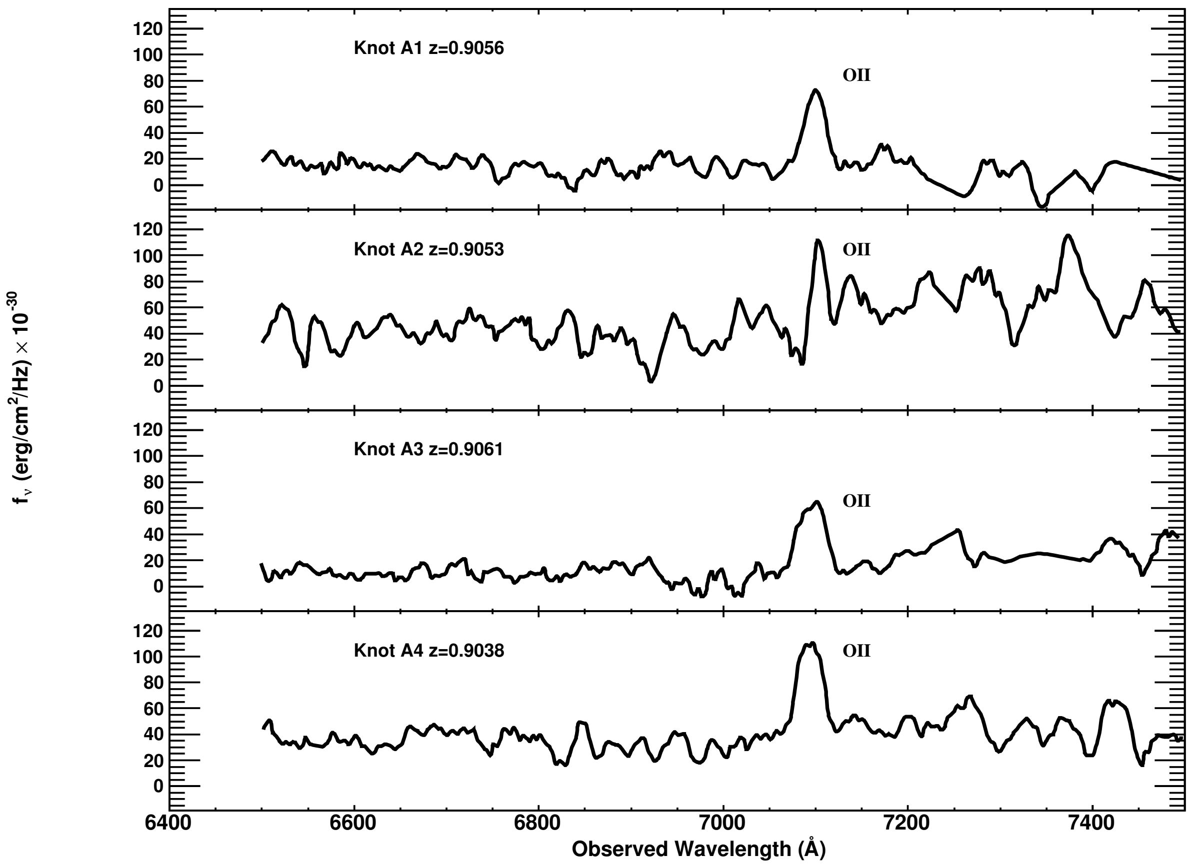

A single emission line which is identified as [OII] 3727Å

Redshift
z = 0.9052±0.0005

Photometric redshift was estimated as
z ≈ 0.7

Elliot Arc Lens Modeling

- Use the r-band image as it has the best seeing
- Subtract off the other objects using GALFIT
- We can identify 8 images which suggest that there might be more than one source being lensed. Assign images 1,4,6,8 to one source and 2,3,5,7 to the other source

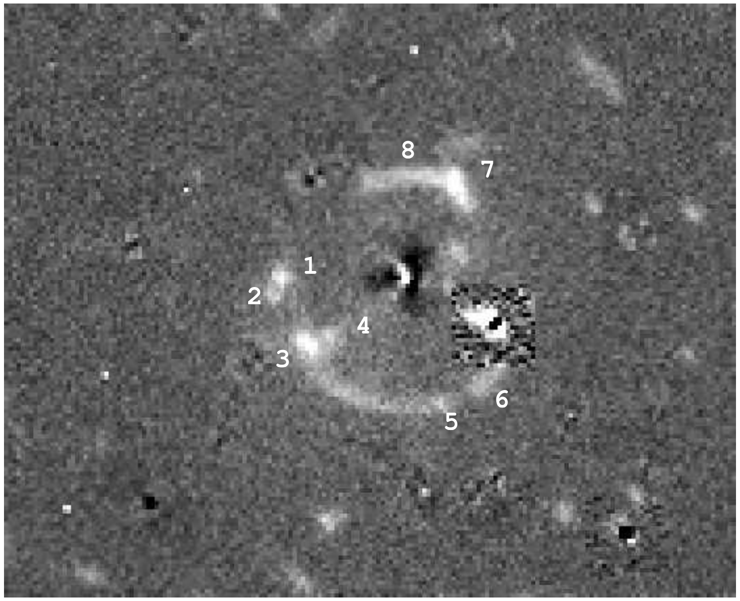

Lens Model

- Use lensmodel
- Use an NFW profile for the dark matter (Navarro, Frenk and White which is a common universal density profile for dark matter halos

$$\rho(r) = \frac{\rho_s}{(r/r_s)(1+r/r_s)^2}$$

- Model the cluster galaxy members using a pseudo-Jaffe profile where r_c is the core radius and r_t is the truncation radius

$$\rho \propto \left(r^2 + r_c\right)^{-1}\left(r^2 + r_t\right)^{-1}$$

- Fix positions, ellipticities and angles from GALFIT
- Allow r_c , r_t and σ_0 (velocity dispersion) to scale according to the luminosity of the galaxy. σ_0 Scaling depends on the mass to light ratio M/L. Fit for r_s, κ, M/L

Results

- **Best fit is for M/L = 4**
- **χ^2 = 0.7 per dof**
- **NFW parameters** $r_s = 10.94''^{+11.68}_{-6.21}\ ,\quad \kappa = 0.452^{+0.663}_{-0.20}$

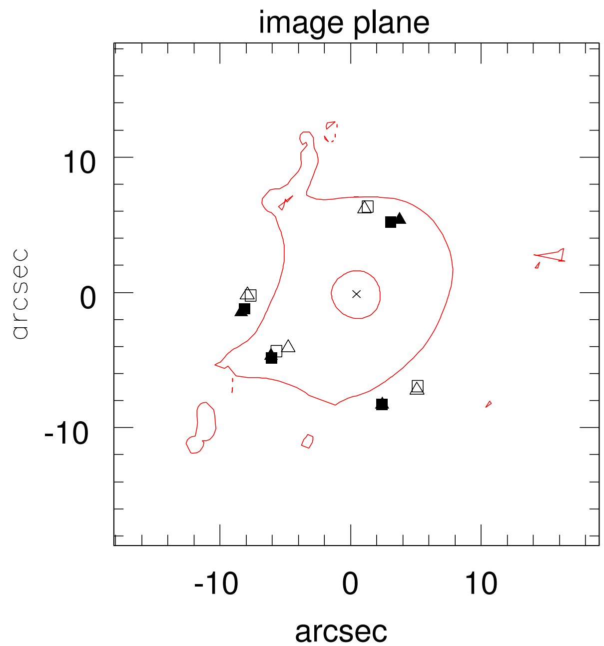

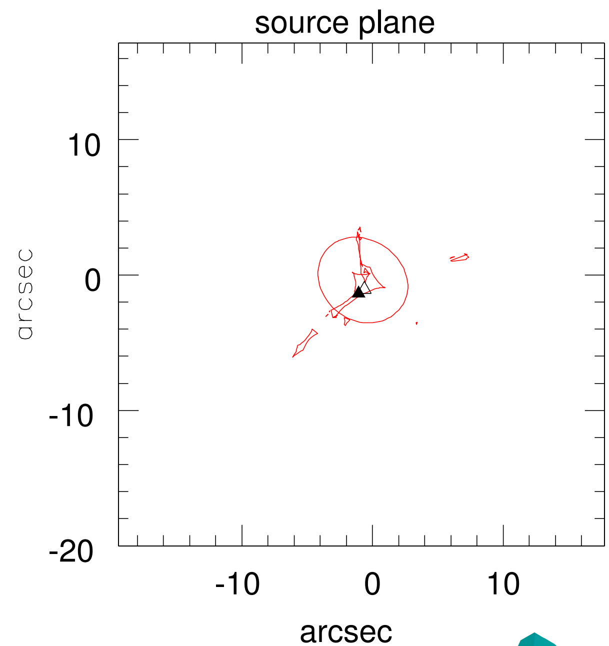

κ Map

Map of $\kappa = \Sigma / \Sigma_{crit}$

Mass inside the Einstein Radius = 1.45 × 10^{13} $M_{\odot}$

Mass due to the NFW profile alone = 1.14 × 10^{13} $M_{\odot}$

Magnification
Source 1 32.46
Source 2 28.77

Paper is in preparation

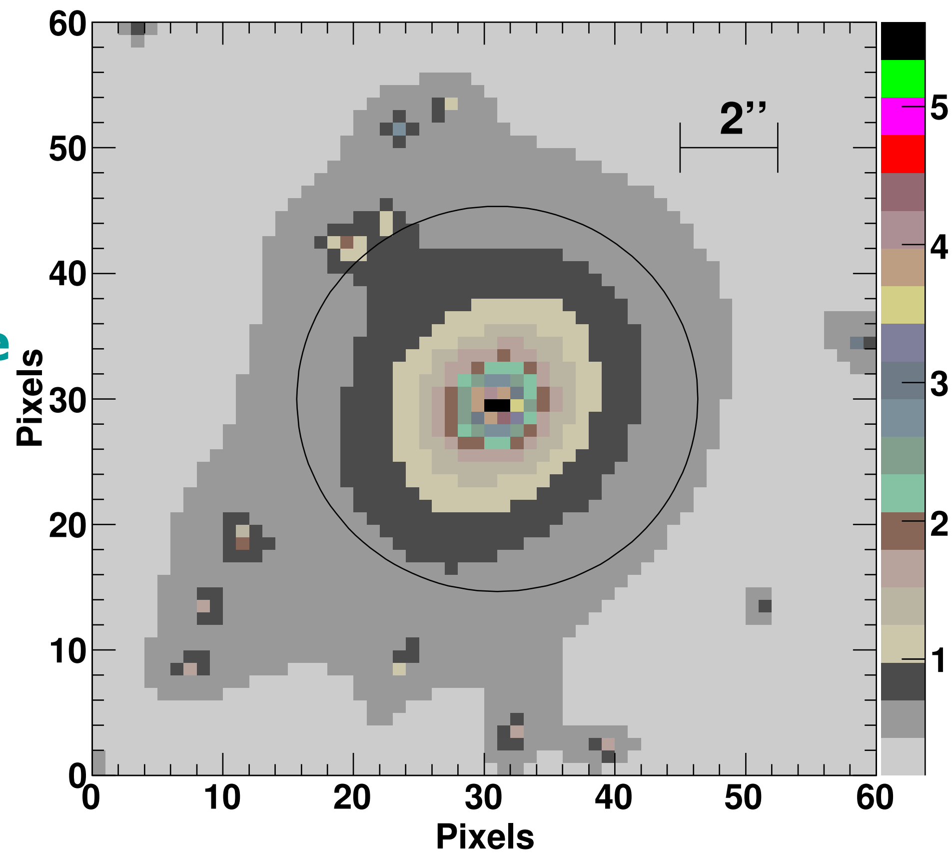

Measuring Weak lensing in clusters

- For each galaxy we define ellipticity components e_1 and e_2

$$e_1 = \frac{I_{xx} - I_{yy}}{I_{xx} + I_{yy}}, \quad e_2 = \frac{2I_{xy}}{I_{xx} + I_{yy}}$$

- I_{xx} etc are the 2nd order moments of the galaxy
- The quantity we want to measure is the tangential shear γ_t which is the component of the shear tangential to an imaginary circle centered on the cluster and running through the source

$$e_t = e_1 \cos(2\beta) + e_2 \sin(2\beta)$$
$$e_c = -e_1 \sin(2\beta) + e_2 \cos(2\beta)$$

- e_c is a control statistic as its value is not affected by lensing

Tangential Ellipticity

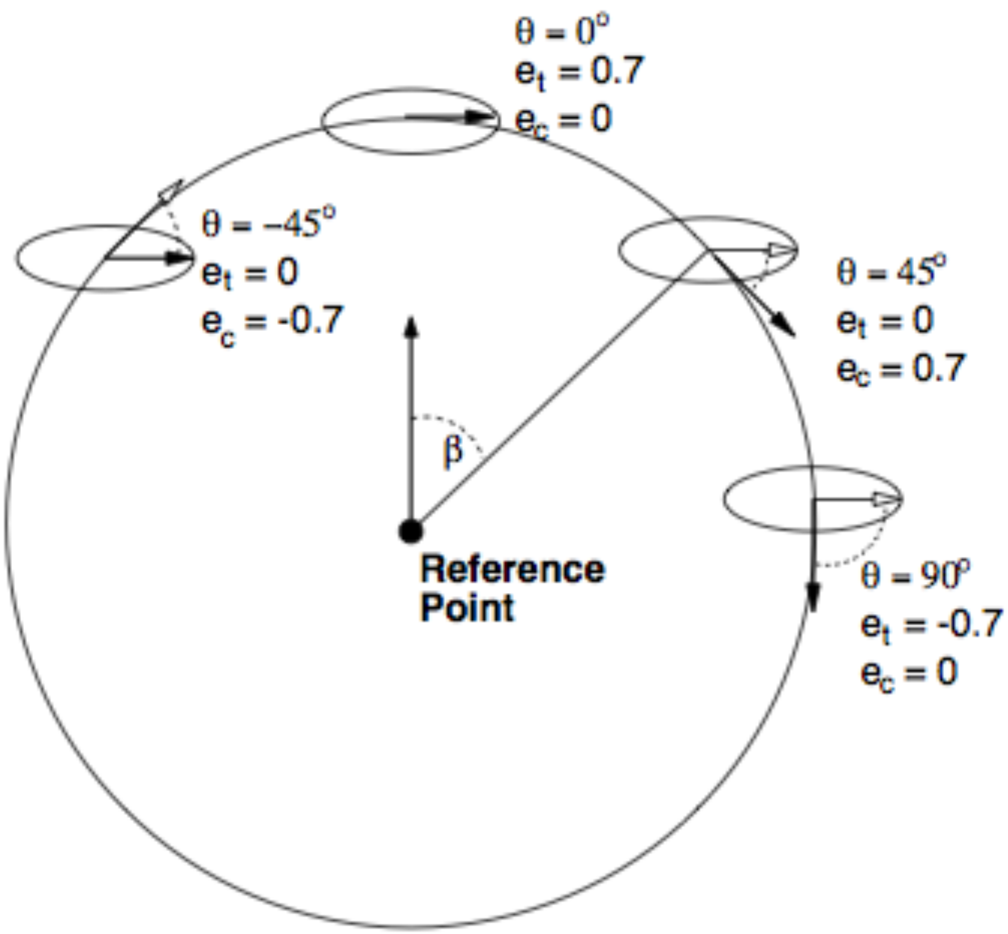

Determining the mass

- We fit an NFW profile to the tangential shear

$$\rho(r) = \frac{\delta_c \rho_c}{(r/r_s)(1+r/r_s)^2}, \quad \delta_c = \frac{200}{3}\frac{c^3}{\ln(1+c) - c/(1+c)}$$

- The fit parameters are the halo concentration c and r_s which are highly correlated
- We define the virial radius $r_{200} = cr_s$ which is the radius inside which the mass density is equal to $200\rho_c$
- The mass corresponding to the radius r_{200} is

$$M_{200} = \frac{800\pi}{3}\rho_c r_{200}^3$$

Elliot Arc i-band weak lensing

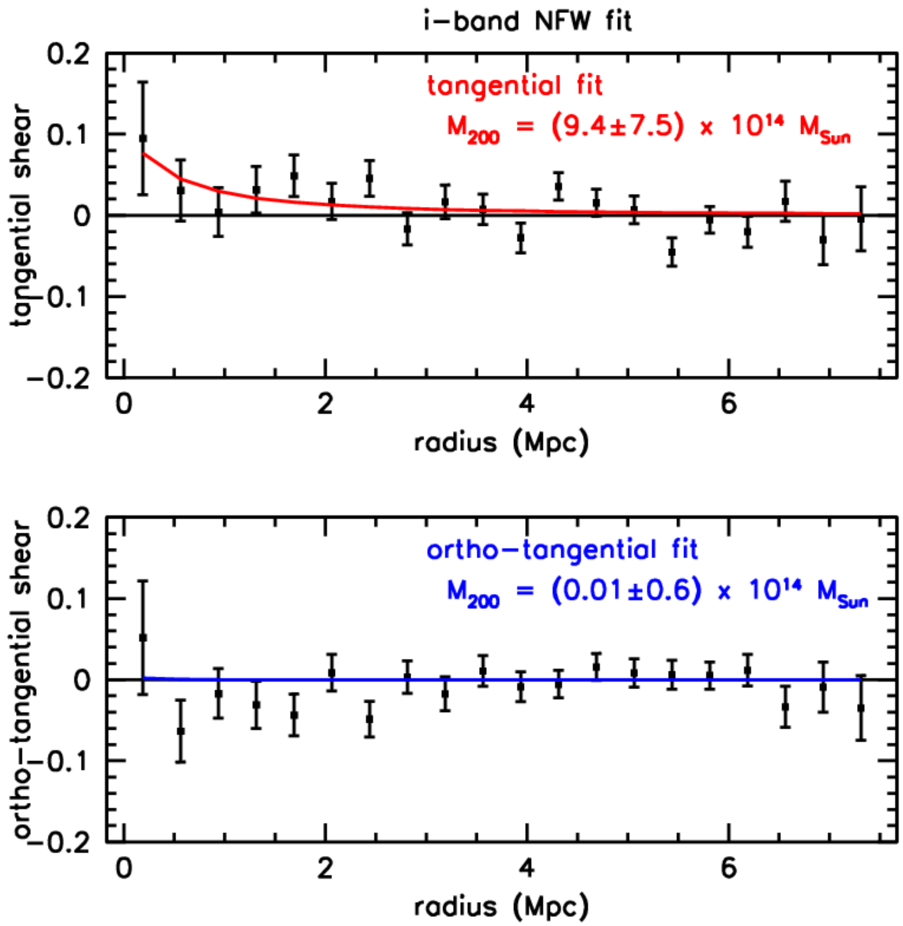

Work done by our intern Emily Drabek

The tangential shear is fit to an NFW profile There is a positive signal but the errors are large. This measurement will be combined with the strong lensing fit to provide an improved constraint on M_{200}

Weak Lensing from the Coma Cluster

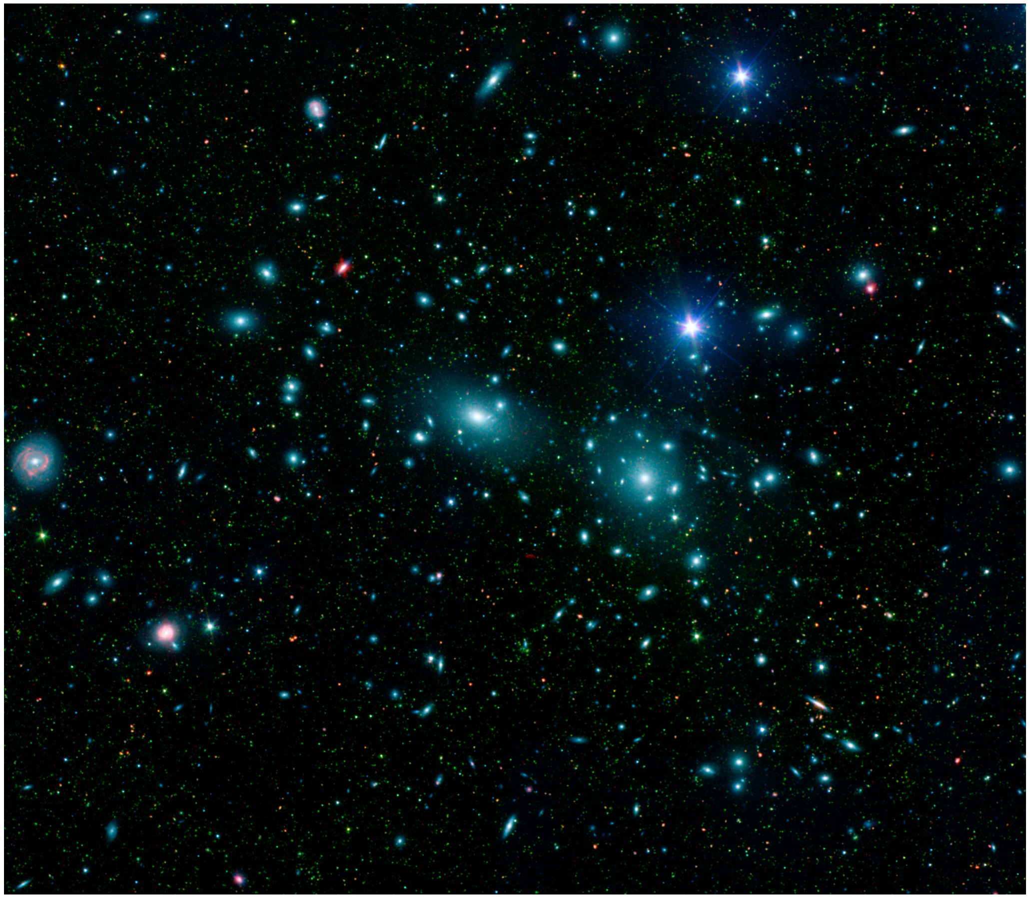

The Coma cluster (Abell 1656) is at a redshift of z=0.02 and contains over 1000 identified galaxies. Due to the low z we can measure a weak lensing signal even with the shallow imaging of SDSS because almost all the background galaxies are at higher redshift than Coma

Kubo et al., 2007 ApJ 671 1466

Weak lensing result from Coma

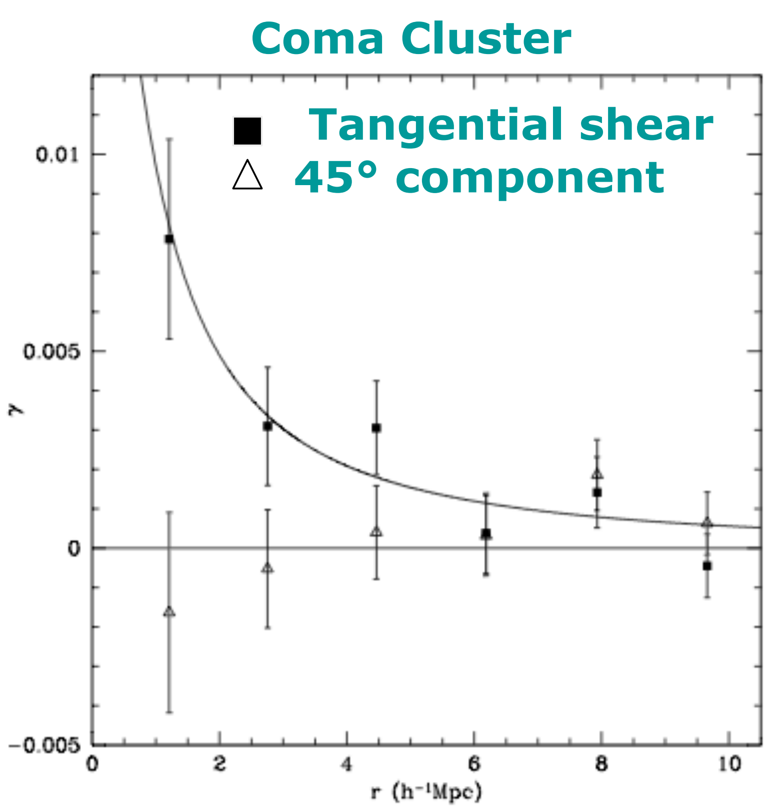

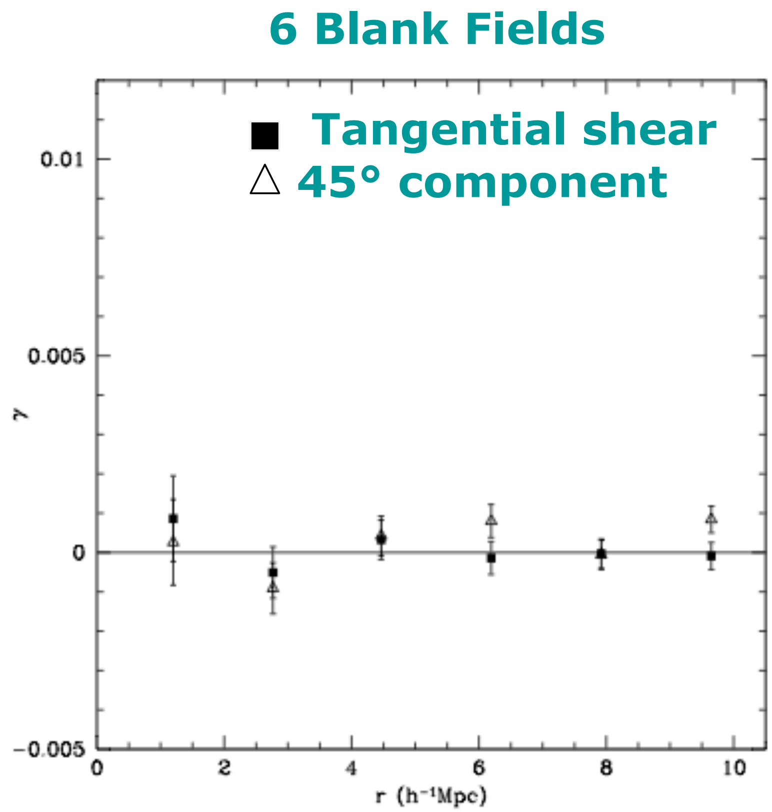

$$r_{200} = 1.99^{+0.21}_{-0.22} h^{-1} Mpc, \quad c = 3.84^{+13.16}_{-1.84}, \quad M_{200} = 1.88^{+0.65}_{-0.56} \times 10^{15} h^{-1} M_{sun}$$

Consistent with other mass measurements to within 2 σ

Weak Lensing of nearby clusters

- Motivated by the Coma measurement we have a program to measure weak lensing signals for other nearby clusters in the SDSS
- This is being done with students from IMSA
- Uses a Mathematica notebook for the analysis
- Kubo et al., 2009 ApJ 702, L110

Cluster Data and Lensing Virial Masses

Name	ID[a]	R.A. (J2000)	Decl. (J2000)	z	$\log(M_{200})$
Abell 1767	3011	204.0347	59.2064	0.0704	$14.34^{+0.28}_{-0.54}$
Abell 2048	8129	228.8088	4.3862	0.0949	$14.78^{+0.22}_{-0.32}$
Abell 2244	3004	255.6771	34.0600	0.0990	$14.46^{+0.30}_{-0.56}$
C4 1003	1003	184.4213	3.6558	0.0771	$14.20^{+0.36}_{-1.17}$
C4 3156	3156	258.8017	64.3191	0.0950	$14.34^{+0.34}_{-0.80}$
Abell 1066	12289	159.7776	5.2098	0.0680	$14.78^{+0.20}_{-0.30}$
Abell 2199	16089	247.1593	39.5512	0.0306	$14.66^{+0.22}_{-0.32}$

Notes. The first five clusters in the table are from the C4 catalog, the last two are from the Berlind catalog. Errors bars on $\log(M_{200})$ are 1σ errors, where M_{200} is in units of $h^{-1}\ M_{\odot}$.

Abell 2244

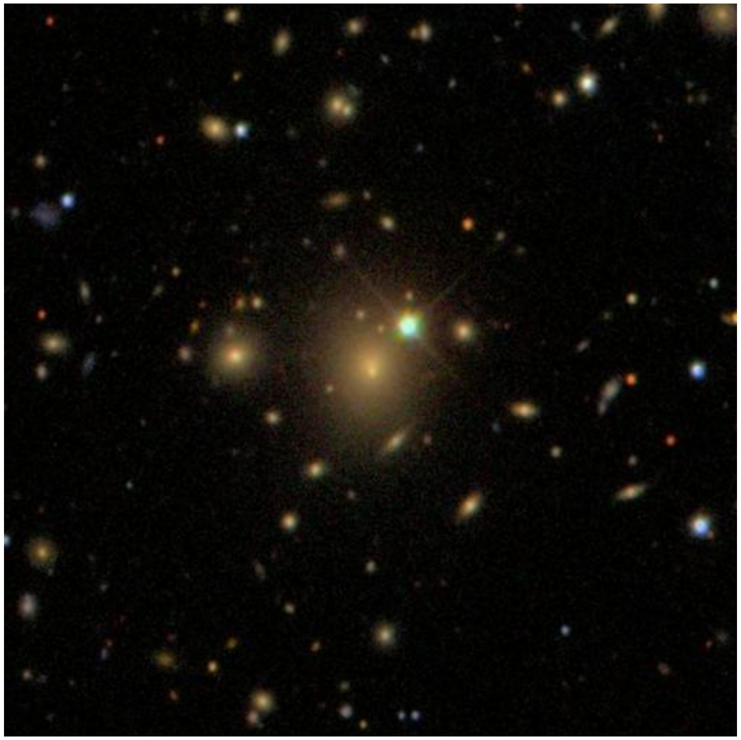

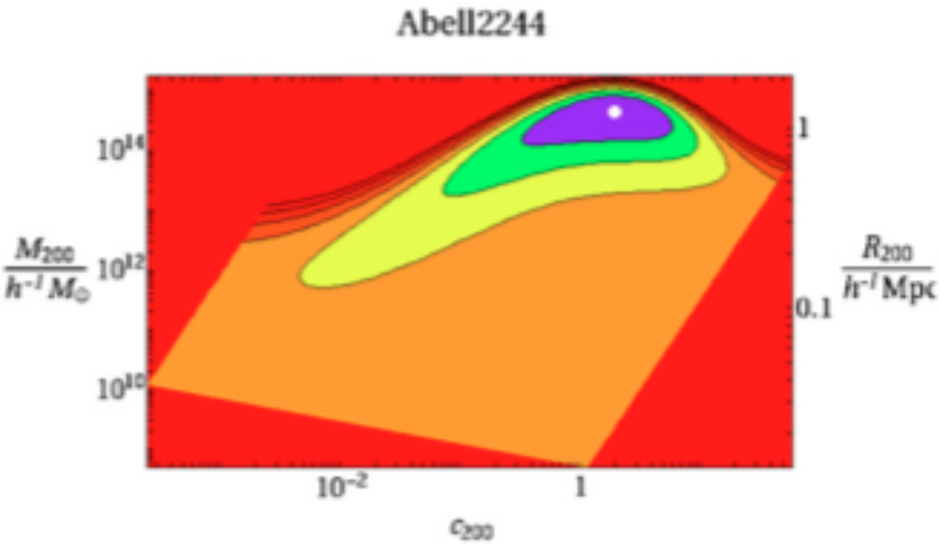

$$M_{200} = 2.88^{+2.87}_{-2.1} \times 10^{14} h^{-1} M_{sun}$$

Future work

- Continue mass modeling using ground-based and HST data - Sahar Allam has a postdoc funded by her HST grant who is working on the HST modeling
- Weak lensing of nearby clusters is an ongoing effort
- Weak lensing in the SSDS Stripe 82 Coadd data is just starting
- Other activities on cluster finding and using clusters to extract cosmology are taking place in the group

Strong Lensing Prospects with the Dark Energy Survey

We can estimate the expected number of strongly lensed systems in the Dark Energy Survey by scaling from other surveys that go to similar depth.

Arc Radius	Number in RCS-2	Number in CFHTLS	Approximate number expected in DES
> 7"		4	243 ± 121
> 5"	29		509 ± 94
3" – 7"		13	789 ± 219
< 3"		22	1335 ± 285

We expect a lot of lenses and the challenge will be to discover them in a more automated way than we do at present
We are starting to think about ways to do this but it is not easy.
The human eye is extremely good at identifying these objects and translating that into software is not trivial

Summary

- We have a very active program of strong lensing studies at FNAL using ground based and HST data
- Have published 6 papers so far with more in preparation
- We have had three HST proposals accepted since 2008 and have just submitted a fourth one
- We also have a very active program of weak lensing studies using SDSS data from both the single pass imaging and the coadded Stripe 82
- We are getting meaningful contributions from IMSA students and interns
- We are preparing for the new data that we will collect with DECam starting in late 2011.